Cleaning of ultra-high temperature milk fouling -Structural and compositionl changes

Hagsten, Carin

2016

Cleaning of ultra-high temperature milk fouling

Structural and compositional changes

PHYSICAL CHEMISTRY | FACULTY OF SCIENCE | LUND UNIVERSITY
CARIN HAGSTEN

Cleaning of ultra-high temperature milk fouling

Structural and compositional changes

Carin Hagsten

LUND
UNIVERSITY

DOCTORAL DISSERTATION

by due permission of the Faculty of Science, Lund University, Sweden.

To be defended at lecture hall C, Kemicentrum, Lund

Tuesday the 8th of March 2016, at 09:30

Faculty opponent

Professor Ian Wilson

University of Cambridge, Cambridge, UK

Organization

LUND UNIVERSITY

Faculty of Science, Department of Chemistry,

Division of Physical Chemistry

Author: Carin Hagsten

Document name

Doctoral Dissertation

Date of issue
2016-03-08

Sponsoring organization

SP Technical Research Institute of Sweden,
Tetra Pak Processing Systems, Arla Foods,
The Swedish Research Council Formas,
The Swedish Farmers Foundation for Agricultural Research (SLF),
The Swedish Governmental Agency for Innovation Systems Vinnova,
Livsmedelsföretagen, and Svensk Dagligvaruhandel

Title and subtitle: Cleaning of ultra-high temperature milk fouling – Structural and compositional changes

Fouling is the deposit of proteins and minerals formed on equipment surfaces during the heat treatment of dairy products. The concentrations of the components and the structure of the fouling reflect the processing conditions used. The use of a higher processing temperature, e.g., ultra-high temperature (UHT) treatment, promotes a mineral-rich fouling. The fouling layer decreases the transfer of heat from the heating medium to the dairy product. A product that undergoes insufficient heating during processing may contain viable microorganisms, which spoil the product and can be hazardous to the consumer. Therefore, an efficient and cost-effective cleaning process is crucial for maintaining food safety, as well as for optimizing energy expenditure. The main goal of this PhD thesis work has been to understand the fundamental mechanisms underlying cleaning for the removal of mineral-rich fouling, which to date has not been fully elucidated. The current investigations into the cleaning process, as well as the structure and chemical composition of the fouling layer reveal that the fouling of UHT processes has a high mineral concentration and low protein concentration. However, the proteins were found to be extensively interconnected with the fouling matrix and to play a crucial role in cleaning efficiency. Cleaning is one of the major processes in the processing of dairy products. The cleaning has to be efficient, always resulting in a clean surface. It is crucial to remove the fouling from the heated surfaces. In this study, cleaning efficiency is shown to be affected by several parameters, such as temperature, alkali cleaning agent concentration, flow velocity, and time. The focus is on the alkali cleaning process, since the acid cleaning is shown to be a rapid process so the gains achieved through optimization of the process parameters are less impressive. Increasing the temperature and the concentration of cleaning agent is shown to have the largest effect on the depolymerization of the protein network within the mineral matrix and therefore has the greatest impact on cleaning efficiency.

Key words: UHT milk fouling; cleaning mechanisms; mineral deposit; protein degradation; cleaning model

Classification system and/or index terms (if any)

Supplementary bibliographical information

Language: English

ISSN and key title

ISBN: 978-91-7422-429-0

Recipient's notes

No of pages: 166

Price

Security classification

Signature 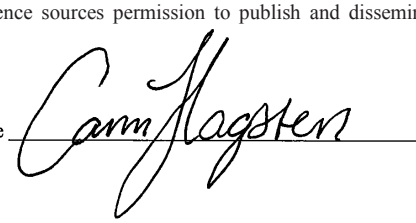 Date 2016-01-27

Cleaning of ultra-high temperature milk fouling

Structural and compositional changes

Carin Hagsten

Cover: Picture of dried UHT fouling layers.

Faculty of Science, Department of Chemistry
ISBN 978-91-7422-429-0

Printed in Sweden by Media-Tryck, Lund University
Lund 2016

“Our greatest weakness lies in giving up. The most certain way to succeed is always to try just one more time.” - Thomas A. Edison

Table of Contents

List of papers included in the thesis

I C. Hagsten, N. Loren, L. Hamberg, J. Wiklund, F. Innings, L. Nilsson, M. Paulsson, C. Trägårdh, and T. Nylander. 2013. **A novel fouling and cleaning set-up for studying the removal of milk deposits produced during UHT-treatment.** Proceeding of the International Conference on Heat Exchanger Fouling and Cleaning, 2013 (Peer-reviewed, www.heatexchanger-fouling.com). June 09-14, 2013, Budapest, Hungary (eds. M. R. Malayeri, H. Müller-Steinhagen, A. P. Watkins), pp 457-464.

II C. Hagsten, A. Altskär, S. Gustafsson, N. Loren, L. Hamberg, F. Innings, M. Paulsson, and T. Nylander. 2016. **Composition and structure of high temperature dairy fouling.** Food Structure 7, pp 13-20

III C. Hagsten, N. Loren, L. Hamberg, F. Innings, M. Paulsson, C. Trägårdh and T. Nylander. 2016. **Removal of UHT dairy fouling - optimizing the process by controlling the protein network degradation.** Submitted to Journal of Food Engineering

IV C. Hagsten, A. Altskär, S. Gustafsson, N. Loren, L. Hamberg, F. Innings, M. Paulsson, and T. Nylander. **Structural and compositional changes during UHT fouling removal – Mechanisms of the cleaning process.** Manuscript

The author's contribution to the papers

I	The author was responsible for the experimental plan and performance of all experiments. Main part of analysis and writing of the manuscript was performed by the author.
II	The author was responsible for the design, experimental work and writing of the manuscript. The scanning electron microscope instrument was run by Annika Altskär.
III	The author was responsible for the design, experimental work and writing of the manuscript.
IV	The author was responsible for the design, experimental work and writing of the manuscript. The scanning electron microscope instrument was run by Annika Altskär. Mathematical modelling was performed by Professor Christian Trägårdh

Abstract

Fouling is the deposit of proteins and minerals formed on equipment surfaces during the heat treatment of dairy products. The concentrations of the components and the structure of the fouling reflect the processing conditions used. The use of a higher processing temperature, e.g., ultra-high temperature (UHT) treatment, promotes a mineral-rich fouling.

The fouling layer decreases the transfer of heat from the heating medium to the dairy product. A product that undergoes insufficient heating during processing may contain viable microorganisms, which spoil the product and can be hazardous to the consumer. Therefore, an efficient and cost-effective cleaning process is crucial for maintaining food safety, as well as for optimizing energy expenditure.

The main goal of this PhD thesis work has been to understand the fundamental mechanisms underlying cleaning for the removal of mineral-rich fouling, which to date has not been fully elucidated. The current investigations into the cleaning process, as well as the structure and chemical composition of the fouling layer reveal that the fouling of UHT processes has a high mineral concentration and low protein concentration. However, the proteins were found to be extensively interconnected with the fouling matrix and to play a crucial role in cleaning efficiency.

Cleaning is one of the major processes in the processing of dairy products. The cleaning has to be efficient, always resulting in a clean surface. It is crucial to remove the fouling from the heated surfaces. In this study, cleaning efficiency is shown to be affected by several parameters, such as temperature, alkali cleaning agent concentration, flow velocity, and time. The focus is on the alkali cleaning process, since the acid cleaning is shown to be a rapid process so the gains achieved through optimization of the process parameters are less impressive. Increasing the temperature and the concentration of cleaning agent is shown to have the largest effect on the depolymerization of the protein network within the mineral matrix and therefore has the greatest impact on cleaning efficiency.

Populärvetenskaplig sammanfattning

Mjölk värmebehandlas för att döda eventuella bakterier och för att förlänga hållbarheten på produkten. Samtidigt som eventuella bakterier förstörs av värmen så sker även andra reaktioner i mjölken. Proteiner förlorar sin naturliga struktur och börjar sätta ihop sig i olika aggregat och formationer som sedan kan fastna på den värmande ytan. Tillsammans med proteinerna fastnar även mineraler, främst då kalciumfosfat.

När mjölk processas i mejeriindustrin bildas fouling på de värmande ytorna. Fouling är en beläggning som byggs upp av en blandning av proteiner och mineraler. Anledningen till att dessa fastnar på ytorna är att de reagerar på värmen i anläggningen. Beläggningen hindrar värmen från att transporteras in i mjölken och måste därför diskas bort innan den blir för tjock, för att försäkra att all mjölk värms upp till samma temperatur.

Kalcium som finns i hög koncentration i mjölk har en egenskap som gör att den löser sig mindre och mindre när temperaturen i mjölken höjs. Därför återfinns en ökad mineralkoncentration i fouling som producerats vid höga temperaturer. Den fouling som har studerats i detta arbete är producerad vid vad som brukar kallas för ultra-hög temperatur eller UHT. UHT-mjölk har en lång hållbarhet och kan förvaras i rumstemperatur. I Sverige finner man den främst i olika typer av kaffemjölk. Strukturen och sammansättningen på den fouling som bildas under denna värmeprocess har noga studerats i projektet för att bättre förstå vad som händer under rengöringen av processanläggningen.

Genom att studera vad som händer under diskprocessen kan förståelse nås kring hur processen kan påverkas och optimeras. De viktigaste parametrarna att förstå är vid vilken temperatur som det är bäst att diska, hur snabbt disklösningen måste flöda över beläggning, vilken koncentration disklösningen behöver ha och hur lång tid som behövs för att ytan ska bli ren. Genom att justera dessa parametrar går det att minska användningen av energi, vatten och diskkemikalier.

En disk i mejeriindustrin sker ofta i två steg. Först används en basisk disklösning för att bryta ner proteinerna och sedan en syra för att ta bort mineralerna som finns

i beläggningen. I detta projekt har det visats att det är av yttersta vikt att det första disksteget bryter ner proteinnätverket i foulingen för att ytan efter disk ska bli ren. En ökad temperatur under första disksteget minskar tiden som krävs för att diska rent. Även en ökad koncentration av disklösningen minskar tiden, men inte med riktigt lika mycket. Det har också visats i projektet att vid just den här typen av beläggning, så har hastigheten på diskvätskan ingen större betydelse.

Resultatet av arbetet är användbart för industrin för att kunna skräddarsy ett system för disken som är mest effektiv för just den anläggningen och den speciella produkten, för att kunna spara energi och optimera användningen av kemikalier, tid och energi.

Abbreviations

BSE	Back scattered electron
CIP	Cleaning in place
CLSM	Confocal laser scanning microscopy
DP	Degree of Polymerization
DCPD	Dicalcium phosphate dihydrate
EDX	Energy dispersive x-ray
HAP	Hydroxyapatite
ICP-OES	Inductively coupled plasma optical emission spectroscopy
LCA	Life cycle assessment
MFGM	Milk fat globule membrane
OCP	Octacalcium phosphate
pI	Isoelectric point
Re	Reynold number
SAXS	Small angle x-ray scattering
Sc	Schmidt number
SE	Secondary electron
SEM	Scanning electron microscopy
Sh	Sherwood number
SSD	Solid state detector
TCP	Tricalcium phosphate
UHT	Ultra high temperature
WAXD	Wide angle x-ray diffraction

WPC	Whey protein concentrate
WPI	Whey protein isolate
α-LA	α-Lactalbumin
β-LG	β-Lactoglobulin

Notations

Latin Letters

Symbol	Unit	Description
c	mol/dm^3	concentration
d	Å	Bragg reflection spacing
D	cm^2/s	Diffusion coefficient
E_a	J/mol	Activation energy
F	1.53	Laser triangulation sensor correction factor
h	W/m^2K	Convective heat transfer coefficient
J or N_A	mol/m^2s	Molar flux
k	W/mK	Conductive heat transfer coefficient
k_c	m/s	Mass transfer coefficient
L	m	Thickness, length
q	W	Rate of convective heat transfer
Q	$Å^{-1}$	Momentum transfer
R	8.314 J/Kmol	Gas constant
R_F	m^2K/W	Thermal resistance of fouling
T	K	Temperature
U	W/m^2K	Overall heat transfer coefficient
v	m/s	velocity

Greek Letters

Symbol	Unit	Description
θ	°	Diffraction angle
λ	nm	Wavelength
μ	kg/ms	Dynamic viscosity
ρ	kg/m^3	Density

1 Introduction

Milk and other dairy products are an important part of the human diet. Milk has high nutritional value and is a valuable complement in a varied diet [1]. The main sources of non-human milk for human consumption are the cow, goat sheep and buffalo, with cow milk representing 83% of the world's milk consumption. In 2014 the production of milk was 802 million tons, corresponding to approximately 110 kg of milk per person in the world [2].

Milk for consumption generally needs to be processed in order to keep the product safe, but also to have a shelf life that allows for distribution of the product and for maintaining the desired properties of the product until it reaches the consumer. One particularly important technique in the processing of dairy products is therefore heat treatment. The heat treatments used for milk differ in terms of the duration and temperature and one of the most intense heating processes is the ultra-high temperature (UHT) treatment, which allow for a long shelf life also at room temperature. The possibility to store milk at room temperature is considered more important in certain areas of the world, especially in areas where maintaining the cold chain from the factory to the consumer is problematic [3].

Heat treatments have some negative effects that are related to the impact of heat on the components of the milk. Proteins, minerals, fats, and carbohydrates are all affected by the increased temperature, even though the overall nutritional value of the milk is not severely affected. However, on the heated surfaces of the equipment used for milk processing, a layer of deposit is formed, called fouling. Fouling reduces the crucial heat transfer to the dairy product.

Since the fouling needs to be removed, the equipment is regularly cleaned. The cleaning process needs to be monitored carefully, as it crucial that the surfaces are clean at the end of the cleaning process and also because the cleaning represents a significant proportion of the total energy consumed in the dairy plant [4]. Cleaning presents a major challenge for the dairy industry, as it is time-consuming and imposes a major environmental burden in terms of the consumption of freshwater, waste-water, chemicals, and energy. The amount of water consumed during

cleaning is high, at approximately 0.5–5.0 liters of water per liter of milk processed [5]. A significant improvement in environmental impact, in terms of decreased usage of energy, water, and detergents, can be achieved by optimizing cleaning protocols. If the time of cleaning could be decreased, the effective production time could be increased. Concerns regarding the environmental impact from the dairy sector are growing worldwide; the International Dairy Federation IDF produced a report in 2015 describing the carbon footprint and the life cycle assessment (LCA) of the dairy industry, including all steps from the primary production to the final product. Whereas the primary production of milk is the main contributor to the carbon footprint, water usage, waste water treatment, usage of chemicals, and energy consumption are parameters that are weighed in the LCA [6].

1.1 Hypothesis

The removal of fouling during the cleaning of process equipment in milk production facilities is highly dependent upon the nature of the fouling. The fouling appears and behaves differently depending not only on the product that is being processed, but also on the time and temperature profiles during processing. The overall hypothesis of this thesis is that a model that can be used to understand and explain the mechanisms that are important for the cleaning process is best achieved by studying the fouling type of interest.

The focus of this work is the fouling produced during ultra-high temperature (UHT) treatment of milk. This type of fouling is known to have a hard and gritty surface and to differ drastically from the fouling associated with the milk pasteurization process, which has been investigated much more extensively. Our specific hypothesis is that the UHT fouling layer behaves in a different way than pasteurization fouling, and that understanding the structure and composition of the layer will hold the key to tailoring an efficient cleaning procedure for UHT fouling.

1.2 Aim

The key questions addressed in this thesis relate to the mechanisms that limit the removal of deposits during the cleaning of equipment used in the ultra-high temperature treatment of milk. In seeking to answer these questions, the focus is on the different process parameters, detergent properties, and the composition and structure of the fouling deposit. The overall goal is to fill the gaps in our current understanding of the mechanism underlying the cleaning process in the dairy industry. While the mechanisms of cleaning for fouling derived from dairy products processed at temperatures <100°C are relatively well understood, the removal of high-temperature fouling has proven to be challenging to study in sufficient detail under relevant conditions. This thesis aims to relate the removal of the fouling layer to its structure and composition, as well as to identify and determine the key mechanisms that control the cleaning process. The objectives of this thesis are:

1. To determine the composition and structure of the fouling/soil matrix.
2. To determine the process parameters that controls the cleaning rate.
3. To establish a comprehensive model that describes the mechanism of the cleaning process.

1.3 Structure of the thesis

This thesis is based on the four attached papers. First, the main theory of the fouling of milk will be presented in Chapter 2. The experimental work performed and the results will be presented in the subsequent three chapters:

Chapter 3: Structure and composition of fouling in dairy processing plants (Papers II and IV)

Chapter 4: Production of UHT milk fouling (Paper I)

Chapter 5: Cleaning of UHT milk fouling (Papers III and IV)

The main findings of the thesis will be summarized and discussed at the end of the thesis. The concluding sections will also include future aspects in terms of applications and the industrial relevance of this work.

2 Processing of dairy products and the concept of fouling

Most milk products are heat-treated before consumption, for several reasons. Milk that is not heat-treated may contain pathogens and other microorganisms that can cause illness if consumed. Some bacteria also produce enzymes, including lipolytic enzymes, which can spoil the product. Thermal processing of dairy products is crucial for ensuring that consumers receive a product that is of high quality and that has a sufficiently long shelf life. [7]

To understand the issue of fouling, a brief introduction as to the processing steps that milk undergoes is needed. The raw milk is filtered when it arrives to the dairy, after which it is either cooled or rapidly heated before cooling. Rapid heating neutralizes some microorganisms, allowing the use of a slightly lower temperature in the subsequent pasteurization step. The milk is then separated into one high-fat or cream fraction and one skim milk fraction.

Part of the cream fraction is homogenized before remixing with the skim milk to obtain the desired fat content. Homogenization is a process in which the fat globules in the milk are broken down into smaller units. The smaller emulsion droplets are stabilized in solution with the aid of proteins together with the phospholipids from the original milk fat globule membrane. Homogenization prevents phase separation of the cream from the skim milk [8].

The milk is thereafter heat-treated to attain the desired shelf life of the product. A combination of heat and time is used in a protocol that involves high temperature for a short time period or a slightly lower temperature for a longer time. In Table 1, examples are provided of the time-temperature relationships used in industry. As treatment at low temperatures does not kill all the bacteria or inactivate all the enzymes present in the milk, spoilage occurs if the cold chain is broken [7].

	Temperature (°C)	Time
LTLT pasteurization	63	30 min
HTST pasteurization	72–75	15–20 s
Ultra pasteurization	125–138	2–4 s
UHT treatment	135–140	a few seconds

Table 1 Examples of time-temperature relationships used for heat treatment in the food industry. LTLT, low temperature for a long time; HTST, high temperature for a short time; UHT, ultra-high temperature. The table is adapted from TetraPak [3].

UHT treatment represents a sterilization process in which not only microorganisms and enzymes are inactivated, but the numbers of viable bacterial spores are dramatically reduced. This process increases the shelf life even further, and since the process is aseptic, room-temperature storage of the product is feasible. UHT treatment involves exposure to approximately 140°C for just a few seconds [3, 7]. UHT treatment can be performed with either direct or indirect heating; indirect heating is achieved with the aid of heat exchangers and direct heating either by steam injection or steam infusion.

As the lethal temperature for the bacteria is reached, many of the milk proteins are denatured and tend to aggregate and precipitate or deposit onto the heated surfaces, forming so-called ‘fouling’. Dairy fouling takes many forms, which are heavily dependent upon the product and the heating process [9]. The major negative effect of fouling is that it decreases the heat transfer from the heating medium to the dairy product. To ensure that enough heat is transferred through the deposit to the milk, the temperature of the heated surface can be increased. However, the fouling layer continues to grow as long as the heating proceeds, and the limit of the heating medium is eventually reached. At this point, the equipment needs to be cleaned [3].

2.1 Fundamentals of heat transfer

To understand the fundamentals of fouling and fouling removal from heated surfaces, it is important look into the process of heat transfer and the impact of the fouling layer. When discussing product heating in the dairy industry, there are different ways of introducing heat into the system. The general system discussed here uses a heating medium (steam or hot water) on the opposite side of a stainless steel wall from the dairy product (Figure 1), so-called 'indirect heating'.

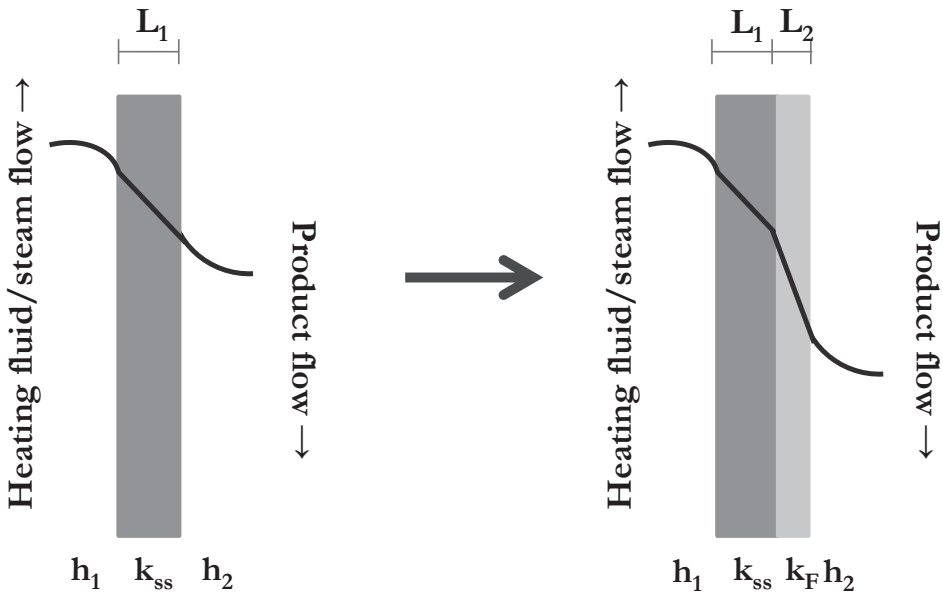

Figure 1 Model of heat transfer through a heat exchanger stainless steel wall. L depicts the thickness of the wall and fouling layer, k is the conductive heat transfer coefficient, and h is the convective heat transfer coefficient.

Heat transfer from the medium to the stainless steel wall, as well as from this wall to the product can be considered as convective heat transfer (Eqns. 2.1 and 2.3), whereas conductive heat transfer occurs through the steel wall (Eqn. 2.2). The heat transfer coefficient k_{ss} is specific for the stainless steel and is usually 16-23 W/mK [10]. The convective heat transfer coefficient through the heating medium and production flow, h_1 and h_2 (W/m^2*K), are dependent upon the fluids used.

$$T_0 - T_1 = q\left(\frac{1}{h_1 A}\right) \quad (2.1)$$

$$T_1 - T_2 = q\left(\frac{L_1}{k_{SS} A}\right) \quad (2.2)$$

$$T_3 - T_4 = q\left(\frac{1}{h_2 A}\right) \quad (2.3)$$

T denotes the temperature (K) in the different zones, q (W) is the rate of heat transfer, A is the cross-sectional area of the heated surface. L is the thickness of the wall. While the fouling is growing on the heated surface the heat transfer capacity through the wall is decreased. The heat transfer coefficient for the fouling layer, k_F, is generally unknown and is also changing with time, since the fouling layer is changing as it grows (4).

$$T_2 - T_3 = q\left(\frac{L_2}{k_F A}\right) \quad (2.4)$$

The overall heat transfer coefficient, U (W/m^2*K), can be introduced for the heat transfer through composite materials:

$$U \equiv q/(A * \Delta T) \quad (2.5)$$

By measuring the overall heat transfer coefficient relative to the value for the clean surface, U_0, the heat transfer coefficient for the fouling layer can be indirectly followed during both fouling and cleaning. In the literature, this is often referred to as the thermal resistance of the fouling, R_F [11].

$$R_F = 1/U - 1/U_0 \quad (2.6)$$

The temperature of the heated surface can be increased to compensate for the loss of heat transfer due to fouling build-up. If the temperature of the heating liquid is increasing it will have an impact on the fouling structure and, consequently, on the cleaning process. The heat-insulating effect of the fouling is exacerbated with increasing fouling layer thickness, and the temperature difference between the heating medium and the product can be used to assess the need for cleaning [3]. It can also be used indirectly to monitor the efficiency of the cleaning process.

When fouling builds up in a tube or on a plate the cross-sectional area available for product flow is decreased. This causes a change in the pressure inside the eqipment, which can also be used to monitor the system and to model the behavior of the fouling [12]. The pressure changes that occur within the system are commonly followed in the industrial setting, as well as in research set-ups that follow the build-up and removal of fouling online [13, 14]. As is the case for changes in heat transfer, the changes in pressure represent an indirect and relative measurements for estimating the removal of fouling.

2.2 Components of milk and their relevance to fouling

Milk components include fats, proteins, carbohydrates, and minerals, all of which are to some extent affected by the heat treatments of pasteurization and sterilization. In this section, the main components of milk are reviewed in terms of their capacities to form fouling during heating.

The chemical composition of the dairy fouling deposit differs depending on the processing conditions, whereby the temperature can vary significantly. Protein-rich (~60%) fouling is produced at lower temperatures, with an onset of about 85°C. This structure has a soft and voluminous character. When the processing temperature is increased the composition of the fouling changes, and at the temperatures used for ultra-high temperature (UHT) processing (137°C-140°C), a dense mineral phase becomes the most prominent feature [14-18].

2.2.1 Proteins

There are five main protein groups in milk: caseins; whey protein; milk fat globule membrane (MFGM) proteins; enzymes; and other minor proteins. The two largest groups will be presented here: whey proteins and caseins. The predominant group of proteins is casein. Cow milk contains approximately 3.3 wt-% protein, with minor seasonal changes due to feed changes and lactation stages [1, 19].

The properties of proteins change drastically with changes in pH and temperature, mainly due to changes in the tertiary and secondary structures of the protein. Not all of the proteins in milk have a secondary structure, which means that they are less sensitive to heat-induced changes in structure/function [20].

Caseins and casein micelles

The caseins in milk account for 80% of the total content of proteins, and 95% of the caseins are assembled into casein micelles, which have an average diameter in the range of 100–200 nm [21, 22]. Casein is a group of four proteins: α_{s1}-casein; α_{s2}-casein; β-casein; and κ-caseins. The α- and β-caseins contain calcium-binding domains that have an important function. The casein micelle prevents the high supersaturated concentration of calcium ions available in milk from precipitating and calcifying the tissues of the cow and the calf. The κ-casein, by virtue of its high degree of hydration of the hydrophilic segment of this amphiphilic molecule, provides colloidal stability for the casein micelle and are located at the outer areas of the micelle [22]. Caseins do not have clear secondary or tertiary structures, which allow some of them to form toxic amyloid fibrils in solution. This does not occur in milk due to the association of casein proteins into casein micelles [20].

The casein micelle differs from a surfactant micelle in that it is much larger and has a highly solvated structure [23]. One of the prevailing theories in relation to the casein micelle structure is that the casein molecules are connected through calcium phosphate nanoclusters, with the κ-caseins protecting it from the outside. Each micelle is thought to contain about 800 nanoclusters [24]. The calcium phosphate nanoclusters, which form an amorphous structure, maintain the integrity of the micelle [20]. It has been shown that when the calcium phosphate is forced to precipitate, e.g., by lowering the pH of the solution, the micelles dissociates and disappears [25]. No drastic changes in casein micelle structure have been observed for temperatures up to 100°C [23]. However, at higher temperatures >100°C, it has been shown that the κ-caseins react with the unfolding β-lactoglobulin (β-LG) and cause instability of the milk solution [26]. This reaction is highly sensitive to changes in pH.

It has been shown that upon heating, the number of calcium phosphate nanoclusters increases, although the nanoclusters do not appear to increase in size. This was demonstrated using Small Angle X-ray Scattering (SAXS) analysis of a sample as the temperature was increased from 5°C to 80°C [27]. At UHT temperatures, polymerization of the caseins is observed, whereby the average particle size increases owing to the formation of larger aggregates. When casein solutions are heated to >120°C, the κ-caseins dissociate from the casein micelle [20] and the micelles may aggregate through calcium phosphate bridging [28].

Initially, casein has been regarded as a hydrophobic protein with a high surface activity, as manifested by its ability to associate into casein micelles. However, it was subsequently shown that denatured whey proteins are more hydrophobic than the caseins and can easily displace any casein attached to a hydrophobic surface, e.g., an oil droplet [29].

Whey proteins

Whey proteins are the second largest group of proteins in milk, corresponding to 20% of the total proteins in milk. The whey proteins have a globular structure and include α-lactalbumin (α-LA), β-lactoglobulin (β-LG), serum albumin, and immunoglobulin, with β-LG being the most abundant [1].

The β-LG monomer contains five cysteine residues, of which four form disulfide bonds in the interior of the folded structure. Cysteine groups are highly reactive and the fifth cysteine residue is available for interaction, if the tertiary structure is partially unfolded. The α-LA has eight cysteine residues, forming four disulfide bonds, and the tertiary structure of the α-LA molecule is also stabilized with a calcium ion [30]. The even number of –SH groups in α-LA explains why the structure tends to readily revert to its original state when cooled down after being heated. Since β-LG generally aggregates with other molecules upon heating, it does not revert to the original conformation upon cooling [31].

When heated, the globular whey proteins go from the native form to an unfolded state, which leads to the formation of aggregates in solution [32, 33]. The intermediate molten globule state occurs under certain conditions and the transition from native to molten globule state is considered to be fully reversible. When the temperature exceeds the denaturation temperature, changes in structure occur and the proteins aggregate. This aggregation involves both specific reactions to form disulfide bridges and non-specific hydrophobic interactions. The aggregation of proteins is also increased if the electrostatic repulsion between protein molecules is screened by an increasing salt concentration. Moreover, the hydrophobic interactions increase with temperature. Additional breakdown of disulfide bonds within the whey protein structure has been observed at treatment temperatures >125°C [32]. Whey proteins are not only sensitive to temperature, but are also sensitive to changes in the pH [34]. β-LG is available as dimers at pH 6.7 and in the form of larger aggregates around the isoelectric point (pI) of 5.1 [9].

The unfolding and aggregation of β-LG at higher temperatures is influenced by the calcium ion concentration. Thermodynamically, ions increase the activation energy for the process that retards the initiation of the process. However, the rate of the reaction, once it is started, is increased due to calcium ion screening of the net negative charges on the protein, thereby reducing the electrostatic repulsion between the aggregating protein molecules [35]. Furthermore, calcium ions can assist in protein unfolding and denaturation by forming cross-links between carboxylic groups, thereby promoting conformational changes. It has also been discussed in the literature whether the whey protein aggregates contribute to fouling formation. Fouling formed from whey protein isolate (WPI) at 85°C did not contain β-LG aggregates, consisting only of unfolding denaturing molecules [36]. The addition of up to 160 mg/L calcium did not have any impact on the protein conformation, as assessed by Raman spectroscopy [36]. However, the level of fouling was increased by the addition of calcium ions to the solution, even at low concentrations [37]. The fouling formed in the presence of a high concentration of calcium is denser and gives a less prominent drop in pressure than a fouling composed of pure protein with a low level of calcium [38].

2.2.2 *Minerals*

The main mineral forming components in milk are potassium, sodium, calcium, magnesium, chloride, and phosphate; in terms of dry matter, the mineral composition is approximately 5.4wt-% [1]. Although some of the minerals in milk, e.g., calcium phosphate, are associated with the casein micelles, significant proportions of the individual minerals are thought to be present in the aqueous phase (one third of the calcium, one half of the inorganic phosphate, and two thirds of the magnesium) [39]. Calcium phosphate is the mineral that plays the most prominent role in fouling deposition and structure.

Calcium phosphate

The concentration of calcium phosphate in milk is above the limit of super-saturation, which means that calcium phosphate would not be soluble in the milk if it did not form complexes with other constituents of the milk. Casein micelles help to keep the calcium phosphate dispersed under these supersaturated conditions. The calcium in the casein micelle is bound to organic phosphor on the phosphoserine groups in the form of calcium phosphate nanoclusters. The calcium phosphor interactions in the casein micelle are important for the stability and

properties of the micelle [39]. Salts of divalent ions, such as calcium, commonly have the characteristic of decreased solubility with increasing temperature [40], and only half of the concentration that is soluble at 20°C is still soluble at 80°C [30, 41]. Upon heating, the calcium phosphate either precipitates or increases the number of nanoclusters in the casein micelles [27].

Calcium phosphate plays a major role during the build-up of milk fouling, at least in the UHT range of production. The formation of mineral-rich fouling at high temperatures may be explained by nucleation theories and the growth of mineral particles in solution. Nucleation is the process whereby a phase transition of solutes in solution causes the formation of seeds of solid particles. Stable species of calcium phosphate, so-called 'pre-nucleation clusters', have been shown to be present in solution, and they participate in the phase transition that leads to the nucleation of particles [42]. Supersaturation of calcium phosphate in solution occurs when the temperature of the milk is increased during the heating process, increasing the concentration above the precipitation concentration (Figure 2). Calcium phosphate particles are then formed until the concentration drops below the precipitation concentration. The precipitate from calcium phosphate can (under certain conditions) be re-dissolved when the solution with precipitate is sufficiently cooled, although when the temperature is high (>90°C) the precipitation cannot be reversed by cooling [30, 39]. During heat treatment at higher temperatures, for example in UHT treatment, the concentration of ionic calcium in milk decreases by 10%–20% [30].

Due to precipitation, the ion concentration decreases and terminates the formation of new particles, although the existing particles will continue to grow until the concentration of ions is below the saturation limit or the temperature of the solution is decreased (Figure 2). In a milk production facility, the continuous flow of new milk maintains a high concentration of ions, and a mono-disperse particle population is expected to form and attach to the surface as fouling. The initial dense fouling layer may be due to nucleation sites in the metal surface that binds mineral-rich structures from the bulk.

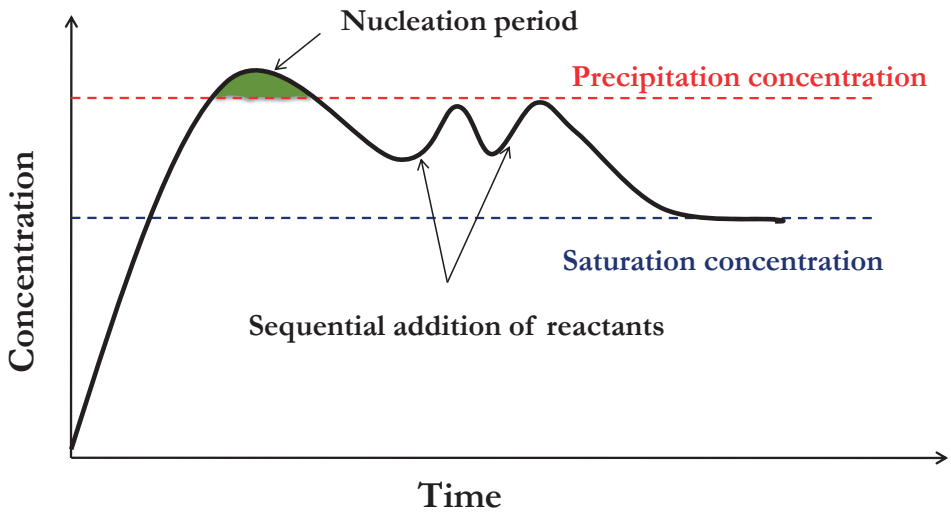

Figure 2 The nucleation process of calcium phosphate. The precipitation of calcium phosphate clusters starts when the ion concentration exceeds the precipitation conentration limit. At calcium phosphate concentrations between the saturation level and the precipitation level, no new clusters are formed, although the existing clusters increase in size. The figure is adapted from [43].

Growth of mineral fouling can also be facilitated by reactions with proteins, whereby the protein clusters aid attachment to the surface [21]. Proteins can also help regulate the particle size of the calcium phosphates. The formation of insoluble calcium phosphate particles during heating in a dairy process often leads to a decrease in pH [9], which alters the properties of the milk. After UHT treatment, the pH has been reported to be decreased by approximately 0.2 units [19, 44]. The level of calcium precipitation is highly dependent upon the pH [26], according to:

$$Ca^{2+} + H_2PO_4 \rightarrow CaHPO_4 + H^+$$

The pH of the product also has an impact on the structure of the fouling formed in the bulk [45, 46]. For example, at pH 6.25, the calcium phosphate forms a needle-like structure of approximately 0.5 µm in length, whereas at pH 6.4, shorter (~0.1 µm) spherical structures are observed. These structures are formed in the bulk and are subsequently precipitated onto the surface [45].

When a pure mineral solution is heated, the calcium phosphate initially covers the surface in a layer of less than 1µm in thickness, and thereafter clusters are deposited on top of this layer. When the layer of minerals is sufficiently thick, larger structural differences can be observed, and the fouling structure is affected by the flow characteristics during production [45].

Inside the casein micelles, the calcium phosphate has a mostly amorphous configuration in the so-called 'calcium phosphate nanoclusters' (CPN), although the precipitated calcium phosphates can be arranged in different structures. Octacalcium phosphate (OCP) and dicalcium phosphate (DCPD/A) are crystalline structures that can be found in nature. In contrast, the different forms of tricalcium phosphate (TCP, Ca/P=1.5) are only found after heat treatment of calcium phosphate solutions and are shown to be present in UHT fouling associated with milk production [17, 39, 47, 48].

2.2.3 Lactose and fat

Lactose is a disaccharide, being composed of galactose and glucose. The concentration of lactose in milk is approximately 4.6 wt-% [19]. For cows, the concentration of lactose is higher early in lactation and decreases with time due to the decreased need for energy supplementation [30]. When added to a solution of whey protein concentrate (WPC) and heated at 95°C, lactose did not have any impact on the level of fouling [40]. However, at high temperatures, lactose will form formic acid, which will lower the pH of the milk and will indirectly change the fouling behavior. Heat treatment of lactose will also cause browning due to the Maillard reaction and will at high temperatures create the somewhat cooked or sweet flavor of UHT milk. The Maillard reaction involves a long series of reactions, starting with the carboxyl group in the lactose or glucose molecule reacting with an amine group on an amino acid, such as lysine, in the milk proteins [49].

While the predominant lipids in milk are the triglycerides (98%), milk also contains phospholipids and cholesterol. The fatty acid composition can vary between batches of milk, and differences in the levels of saturated and unsaturated fatty acids can be seen at different stages of lactation, as well during the different seasons [30]. As most of the lipids found in milk are located in the spherical milk fat globules, milk can be regarded as an emulsion of oil in water [30].

The phospholipids, corresponding to no more than 1% of the total milk lipids, are very important for the microstructure of the fat globules. The phospholipids create the membrane structure that surrounds a triglyceride core [50, 51]. In the fouling that is formed during heat treatment of milk, fat is not found to any significant extent, and since changes in the fat content have not been noted to affect the overall level of fouling [14, 52], they will not be discussed further here.

3 Structure and composition of fouling in dairy processing plants

3.1 Chemical diversity and temperature-dependence of fouling

Two main types of fouling occur in dairy processing equipment during heat treatment of milk: 1) low-temperature fouling, also known as type A (<100°C); and 2) high-temperature fouling, termed type B (>120°C) [14]. The two types of fouling layer are different in appearance; type A is soft and voluminous, while and type B fouling has a hard, gritty surface. In the present study, in the preheating section at type A temperature, the fouling is very thin and translucent. Within the fouling, small islands of the more compact structure, similar to the fouling from the UHT section can be seen (Figure 3). The UHT fouling in this project has a rough structure, and the fouling layer is thicker and harder but becomes brittle when dried. The protein content of the low-temperature fouling is high, at around 60%, although this content is drastically decreased at higher temperatures. The mineral content has the opposite profile of temperature-dependence as compared with the protein content, and the mineral content in the high-temperature fouling is around 70% [14]. This composition is also confirmed in Paper II.

Figure 3 Image showing the low-temperature, protein-rich fouling produced in the pre-heating section (left panel). This fouling type is thin and translucent, whereas the mineral-rich UHT fouling (right panel) is thicker and has a rough surface.

The fouling build-up is dependent upon several factors, one of which is the time-temperature profile of the production unit. It is also known that the pre-treatment step is important in decreasing both the amount of fouling and the rate of fouling formation in the final heating section [14, 16, 40, 52, 53]. The structure of the fouling in this last section is not necessarily changed due to pre-heating, but the amount of protein is reduced [52]. It has been postulated that the fouling that occurs in the final heater initially goes through a lag phase during which the fouling layer is not growing, followed by a more rapid growth phase. The temperature of the preheating step has to be higher than the denaturation temperature of the proteins in the milk to exert any impact on the fouling rate. No lag phase is observed at temperatures in the range of 140°C–150°C in the final heater, and the buildup of fouling is not affected by the pre-heating process [52, 53].

It has been suggested that the fouling build-up is a surface process. Therefore, the fouling structure has an uneven structure with many crevices, which according to the authors would have been filled if bulk aggregates were important for fouling build-up [40]. It has however also been shown that mineral fouling can be formed from clusters in the bulk that are subsequently deposited onto the surface [45]. Furthermore, it has been reported that the fouling layer from milk heated at close to 100°C has a denser bottom layer and a more spongy top layer, with the two layers containing both protein and mineral components [54]. In a previous study, an indication of spatial distribution was observed at 140°C, and the mineral content was somewhat higher close to the metal surface. The fouling surface is no

more than 7 μm thick and did not show any sharp boundary from being mineral-rich to being protein-rich. The authors have proposed that the protein/mineral fouling could be formed simultaneously, and that the minerals located closest to the metal surface could have migrated through the porous structure during the production process [52]. The fouling used in this work is approximately 10 to 100-times thicker, and the analysis of spatial variation of the first few microns was not performed due to limitations inherent to the employed analytical techniques.

The mineral fraction of UHT fouling is substantial, and the crystalline structure of the calcium phosphate that precipitated into the fouling varies with temperature and pH levels. At lower temperatures, determining the structure is challenging, although the crystallinity increases with temperature [39]. As discussed in Chapter 2.2.2, precipitation that occurs at temperatures <100 °C is reversible, whereas the precipitation that occurs at the UHT temperature is irreversible.

As part of the work for this thesis, fouling has been studied using several different methods to reveal both the composition and structure. We have investigated how the composition and structure of UHT fouling change during the cleaning process. Figure 4 provides an overview of the analysis methods used, showing both online (A and B) and offline (1–6) techniques. The online analysis is followed by offline analyses numbers 4 to 6. The techniques are further described as the results obtained are presented in the coming chapters.

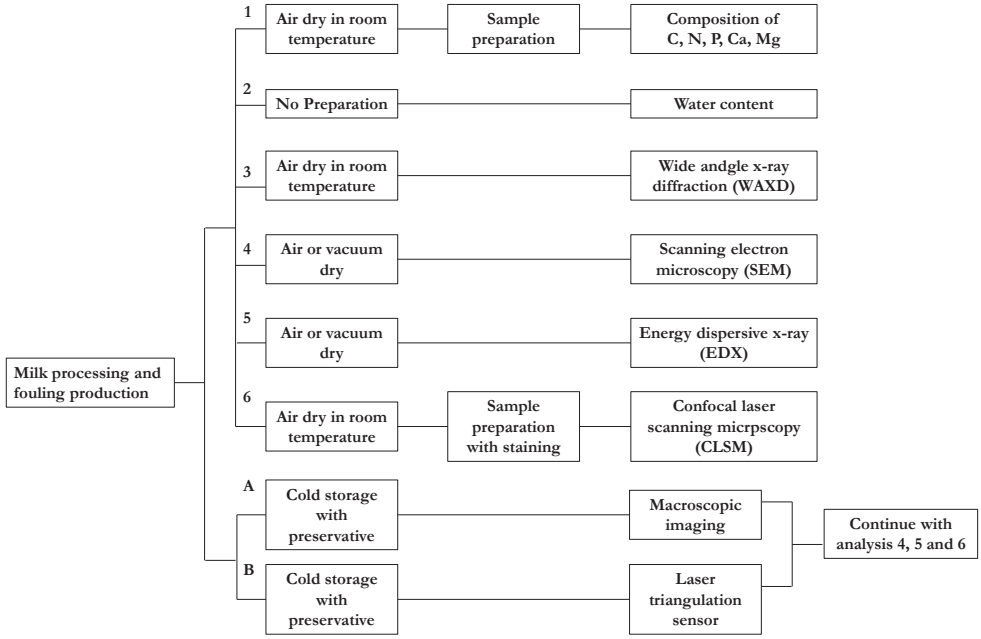

Figure 4 Workflow of the experimental investigations in the work of this thesis. Six offline methods (labeled 1–6) and two online methods (labeled A and B) were used to study the structure of UHT fouling..

3.2 Structure and organization of the fouling layer formed during UHT milk processing

The structure and organization of the UHT fouling was studied using Scanning Electron Microscopy (SEM), Confocal Laser Scanning Microscopy (CLSM), Energy Dispersive X-ray Spectroscopy (EDX), and Wide Angle X-ray Diffraction (WAXD). For information on the equipment used, please refer to Papers II and IV.

3.2.1 *Scanning Electron Microscopy (SEM)*

SEM has previously been used to resolve questions concerning the build-up of fouling and the structures of the protein and mineral networks in the milk deposit [18, 46, 55]. To understand the SEM analysis, a brief introduction to the technique is warranted. The instrument uses a beam of electrons that is scanned over the sample; the electrons are scattered or emitted from the sample back towards a detector, which creates the image.

The two most commonly used signals for forming images in the SEM are the backscattered electrons (BSE) and the secondary electrons (SE). There is a significant difference in the energy levels of the BSE and SE, in that the BSE contain 70%–90% of the original beam energy (typically 10–30 keV) if the material consists of elements of high atomic number (e.g., a metal), while the SE contain beam energy of only 0–50 eV. As the SE are more likely to be reflected to the detector from far away from the first beam of incidence and they are scattered more than the BSE, they have lower energy [56]

The mineral-rich part of the fouling feeds back a strong signal from the BSE, whereas the organic part of the fouling gives a signal of lower intensity. In this project, a relatively high voltage, 20 keV, was used to acquire suitable images of the structure of the fouling layer. The application of a high voltage gives strong penetration and high resolution through the depth of the layer, although it may provide less information on surface details. The image is also affected by the detector, which in this case was a solid state detector (SSD), which tends to give better resolution and contrast as the SE electrons are discarded. A threshold value of 2–5 keV is needed for this type of detector [56].

Two types of initial fouling structures were previously identified from the topography of the fouling layer: mineral crystals and spherical protein aggregates [54]. The UHT fouling studied here has a clear irregular pattern in the morphology owing to the flow along its surface. This phenomenon is observed in both the thinner and thicker parts of the fouling layer.

In Figure 5A, the fouling layer is shown from the top in one area of the surface that features a thinner layer. It is in these areas that we placed the laser triangulation sensor for studying fouling thickness during cleaning. The fouling seems to be form ridges perpendicular to the flow. Close to the metal surface, the fouling layer is dense and flat (Figure 5B). In this case, the fouling layer appears to have been built up from the surface, leaving marks from the mechanical treatment

of the metal coupon on the bottom surface (i.e. that which remains after the fouling layer is detached).

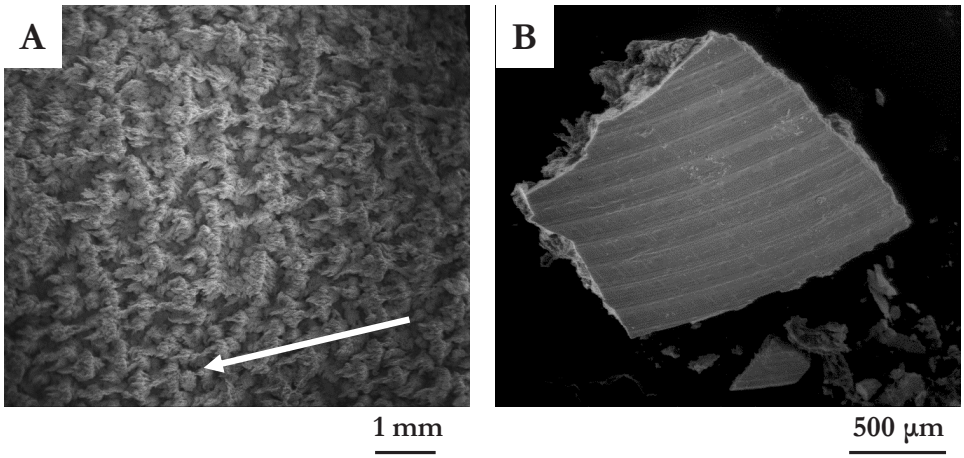

Figure 5 SEM images of the structure of UHT fouling observed from in top view. A, The impact of the flow on the fouling topology; B, view from the bottom of the fouling layer. The bottom of the layer has been in contact with the stainless steel and is smooth and dense. The white arrow indicates the direction of the flow.

The fouling structure and the changes that occur in the fouling structure during cleaning were investigated. Typical SEM images of a cross-section of the fouling layer are shown in Figure 6A. All the cross-sections were prepared by carefully cutting the fouling layer with a sharp razor blade. The UHT fouling produced during 15 hours of run time in a turbulent flow does not exhibit a homogeneous layer thickness for the entire exposed surface area. Instead, the fouling layer thickness varies within the same sample, from around 50 µm to several hundred micrometers.

Both at the top of the structure and further down towards the metal surface the fouling comprises smaller spherical structures (Figure 6B). The shape and organization of these structures suggest that they have not grown out from the fouling surface, but have instead formed as a bulk process and subsequently become attached to the fouling layer. The flow pattern of the process during build-up has been shown to result in a structural difference in the fouling layer along the surface [54]. This involves large variations in thickness and the formation of pillars, which most likely grow as a result of the attachment of bulk aggregates.

The structural analysis with SEM and the confocal laser scanning microscopy (CLSM) analysis reveal that there are areas at the top of the fouling that do not have the same particulate structure as the remainder of the fouling, instead having a smooth surface layer structure. This structure is indicated in Figure 6A. This structure was analyzed and was found to be quite different in terms of its elemental composition from the rest of the layer (Figure 10).

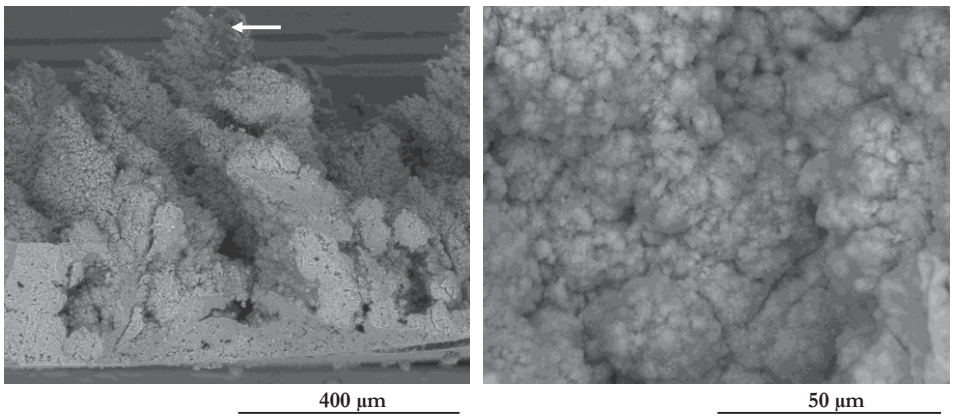

Figure 6 A, SEM image of a cross-section of a layer of UHT fouling formed over a time period of 15 hours. The white arrow indicates a smooth area that is rich in organic material. B, SEM image of the fouling at a higher magnification showing the particulate fouling structure.

3.3 Chemical composition of fouling formed during UHT milk processing

The chemical composition of a fouling layer is of interest, as it will have a significant impact on how the fouling layer behaves when exposed to different cleaning solutions. It is also useful in revealing the spatial variation of the elements in the fouling layer. In this work, several experimental techniques to determine the composition of UHT fouling have been used. For details regarding the experimental set-up of the techniques used please refer to Papers II and IV.

To understand the structure of interest it is important to have a good understanding of the the elements present in the fouling. The bulk concentration of protein and important minerals in the fouling layer was analyzed by measuring the total

carbon, total nitrogen, calcium and phosphorous contents. The mineral part was measured with a technique called Inductively Coupled Plasma-Optical Emission Spectroscopy (ICP-OES) [28, 45]. The chemical analyses in this work were carried out at the Lund University Department of Ecology. The dry samples were sent to the laboratory where they were dissolved in a nitric acid solution. Fouling samples were in this project collected at several processing temperatures (Table 2), even though the UHT fouling was the main interest for the cleaning studies. The high-temperature fouling has a high mineral content and lower protein content, as reported previously [14, 17]. The low-temperature fouling, collected at approximately 100°C, instead has a composition similar to type A fouling, being rich in protein and having a low mineral content. Visual comparison of the samples reveals clear differences in thickness and color between the high-temperature fouling and low-temperature fouling (Figure 3). The low-temperature fouling is thin and translucent, whereas the high-temperature fouling is thick and has an opaque beige coloring. Both the fouling types are brittle, although it is possible to cut the high-temperature fouling with a blade to obtain a clean edge.

The water content of UHT fouling was investigated by determining the weight before and after drying, and was found to be in the range of 40%–60% of the native fouling. The protein content is derived from the analysis of the nitrogen content in the sample. A common practice is to use the so-called Jones factor for milk to calculate the protein content as N*6.38 [57].

	Ca	PO_4	Protein	Ca/P	Water content
Low temperature fouling	18±1	25±1	37±2	1.7	N/A
UHT fouling	27± 2	44± 3	11± 1	1.5	40-60

Table 2 The chemical composition of UHT fouling. The concentrations of calcium, phosphate, and protein are given in wt% of the dry weight of fouling. The water content is given in wt% but in relation to the wet weight of the fouling. The Ca/P ratio is calculated from the atomic percentages of the constituents in the dry samples.

3.3.1 Confocal Laser Scanning Microscopy (CLSM)

CLSM has previously been used to reveal the changes in the microstructures of the food products that are a consequence of processing and to link the microstructure and rheology to the sensory perception of food [58]. The imaging technique relies on fluorescent molecules that are attached to the sample structure. When the fluorescent molecule is attached to the sample, the molecule emits light of a specific wavelength when excited with a laser beam. Information on the composition and structure of the sample can be obtained by using stains that have different excitation and emission wavelengths [59]. In this project, one stain for calcium ions and one for proteins were used, which emit green and red light, respectively. The CLSM gives information regarding the distribution of the different components in the structure, and it can be used as a complement to the information on structures obtained using SEM.

With CLSM, the information on the microstructure of the fouling layer is gathered from thin sections taken at different depths of the sample. Images of these thin sections, recorded in so-called 'focal planes', can then be stacked together to create a 3D image. This concept is visualized in Figure 7. The pixel in the stack with the highest intensity is displayed in the 3D image. The 3D effect is created based on the fact that a pixel that lies deeper in the structure presents a lower intensity even though it has the highest intensity in the stack [60]. Areas of very low intensity in a single section are shown in black, and are interpreted by the brain as being located at the back of the structure when the images are stacked.

Several dyes were tested for staining the protein component of the UHT fouling. Texas Red sulfonyl chloride was the dye chosen for staining the protein component of the fouling layer, and a staining protocol was developed. This dye reacts with primary amines, e.g., lysine, in the protein to form stable sulfonamides. The concentrations of primary amines in casein and whey protein are reduced when heat-treated at 120°–140°C [61], which may influence the fluorescence of Texas Red when used for analyzing UHT fouling. Texas Red is highly reactive and water-soluble, and it is also less stable in alkaline environments [62]. Fouling studies performed after cleaning with alkali solutions show different signal intensities for Texas Red staining, which may be due to residual alkali being solvated in the liquid when the sample is wetted during the staining procedure.

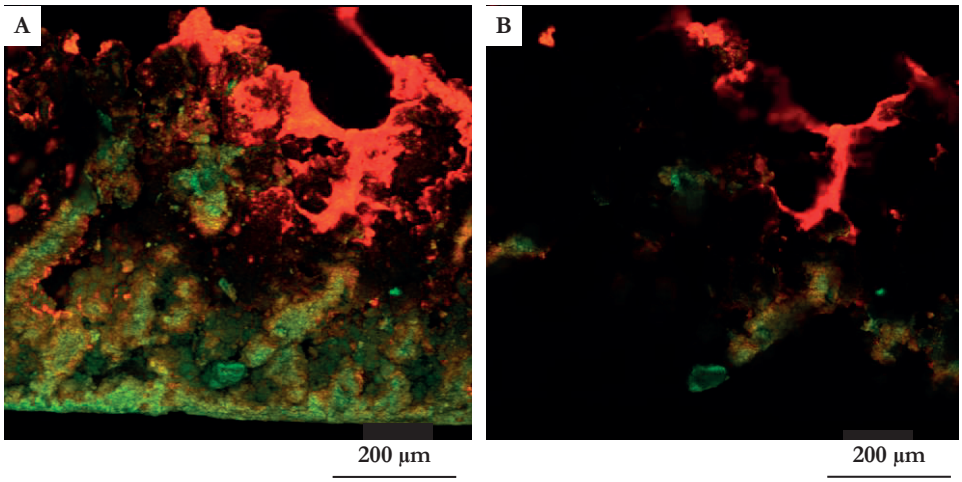

Figure 7 For CLSM, the images were recorded in different focal planes, as shown in B, where only the stucture in focus is visualized. When the focal planes are stacked, a 3D image of the structure is constructed.

When choosing a dye for visualizing the mineral fraction of the fouling layer, one important aspect is to use a dye that has excitation and emission properties that are different from those of Texas Red. The protein dye used is excited at 589 nm and has an emission peak at 615 nm, which is suitable for the use of a Helium/Neon laser. Calcium Green-A1 was chosen as the dye for staining the mineral fraction, as it is excited at 490 nm and has an emission peak at 531 nm, allowing the use of an argon laser source. The Calcium Green-A1 dye has very little autofluorescence and is brighter than other commonly used dyes, such as Fluo-3 [63].

Before considering the CLSM as a method of evaluating the UHT fouling structure, one concern was whether the structure could be kept intact during staining. The stains are liquid-based and the structure should not be altered by the treatment. Wet, air-dried, and freeze-dried samples were analyzed for structural alterations. No significant changes were detected in the structures of the native fouling layers that could be associated with the choice of preparation method. The wet samples were not used for further studies due to difficulties in obtaining reproducible samples, as well as the poor storage stability of these samples. Furthermore, when the fouling was wet it firmly attached to the surface. However, when the samples were dried the fouling layer detached from the coupon metal surface and could easily be transferred to the microscope.

The structure of the UHT fouling was found to be rather robust, which is most likely due to its high mineral content, and the freeze-drying of the samples did not improve the preservation of the structure. However, after a short acid cleaning step, when the mineral structure had been removed, freeze-drying of the sample was found to be crucial for structure preservation. However, the staining of such a sensitive structure was not successful, as the liquid present during staining collapsed the protein network. Therefore, the CLSM technique was not used for the structure/composition analyses after acid cleaning.

For native, non-cleaned, UHT fouling, CLSM provides valuable information regarding the interpenetrating networks of proteins and minerals. Both protein (red) and calcium (green) are dispersed throughout the bulk structure. At a lower magnification, the smooth surface layers are clearly seen in bright red in Figure 7A. The occurrence of these bright-red deposits at the top of the layer warranted further analysis using energy dispersive x-rays (EDX), which confirmed the high concentrations of organic material in these areas (see Chapter 9.3.2). At higher magnifications (Figure 8), calcium clusters surrounded by a protein network are evident. The appearance of these clusters is in agreement with the results of the SEM imaging. In addition, the proteins are surrounding the clusters, which further confirm the existence of an interlinked network of proteins and minerals throughout the UHT fouling layer. The protein network should be relatively easy to access and to degrade by an alkali cleaning process.

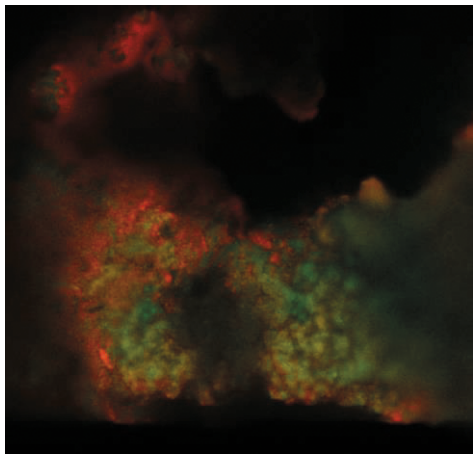

Figure 8 CLSM image of the composition and distribution of calcium and protein in the UHT fouling. The heterogeity of the material makes structural analysis with CLSM challenging, although the interconnectivity of the minerals and proteins is apparent.

3.3.2 Energy Dispersive X-ray Spectroscopy (EDX)

EDX spectroscopy coupled with SEM was used to investigate the variability of the spatial distributions of the different elements in the sample. From the earlier chemical investigation, only the total elemental composition of the UHT fouling was known. EDX has been used previously to study dairy fouling, albeit mainly to look at the growth of the fouling layer during the early stages of the fouling process [55].

As the name suggests, EDX employs the x-rays that are emitted due to ionization of atoms when the electron beam interacts with the sample. The energy levels of the x-rays are characteristic fingerprints of the elements in the material, and can be used for both qualitative and quantitative analyses. The x-rays emitted from the elements with low atomic numbers have low energy; due to absorption effects, both of the material and of the detector, the sensitivity for these elements is reduced [56]. These low-atomic-number elements include nitrogen and carbon, which of course makes the analysis of organic matter from the EDX data from UHT fouling challenging.

The relevant elements for high-temperature dairy fouling are Ca, P, N, O, C and S. The EDX chemical composition data are derived from a sample that has a pear-shaped volume, typically a few microns in diameter and depth. The precise extent of this interaction volume is highly dependent upon a combination of the acceleration voltage of the microscope and the density of the investigated material. To attach samples to the sample holder in the SEM, it is common to use a double-sided sticky tape that is carbon-based. Since carbon is one of the main elements to be studied when it comes to fouling, this tape could not be used. Instead, the sample was mechanically attached by carefully clamping it to the sample holder.

The next issue is how to measure nitrogen. While the level of N is commonly used to calculate the protein content in a sample, it is difficult to use it in this case. The N content of UHT fouling is approximately 2 wt% and this level is not easily detected by the EDX. The trends in spatial variation of the proteins are instead visualized as variations of the carbon content. As there may be carbon-containing components other than protein in the fouling, the more general term of 'organic component' has been applied.

The results regarding the spatial variability of components obtained from the EDX measurements should be regarded as trends, and for this purpose the fouling layer has been divided into three subsections (Figure 9): 1) the bottom layer, which encompasses the area up to a point approximately 50 μm from the metal surface; 2) the interior of the layer; and 3) the top surface. These subsections were designated in the images of the cross-sections of the fouling layers cut for analysis (Paper II, Appendix A).

From the EDX measurements, it can be concluded that there is no significant spatial variation of the calcium component (Figure 9). This concords with the structural images of the fouling layer, showing them to be composed of spherical aggregates. The spherical structures are observed all the way from the lower part of the fouling, close to the metal surface, to the upper part close to the bulk flow. However, closest to the metal surface, the aggregates appear to be sintered. This may be a consequence of the long heat-processing times used during production, although it may also reflect that part of the structure is nucleated at the surface. The aggregates range in size from approximately 5 μm to 20 μm, and since they are expected to contain a high concentration of calcium phosphate together with a smaller amount of an organic component, the presence of casein micelles or caseins cannot be excluded.

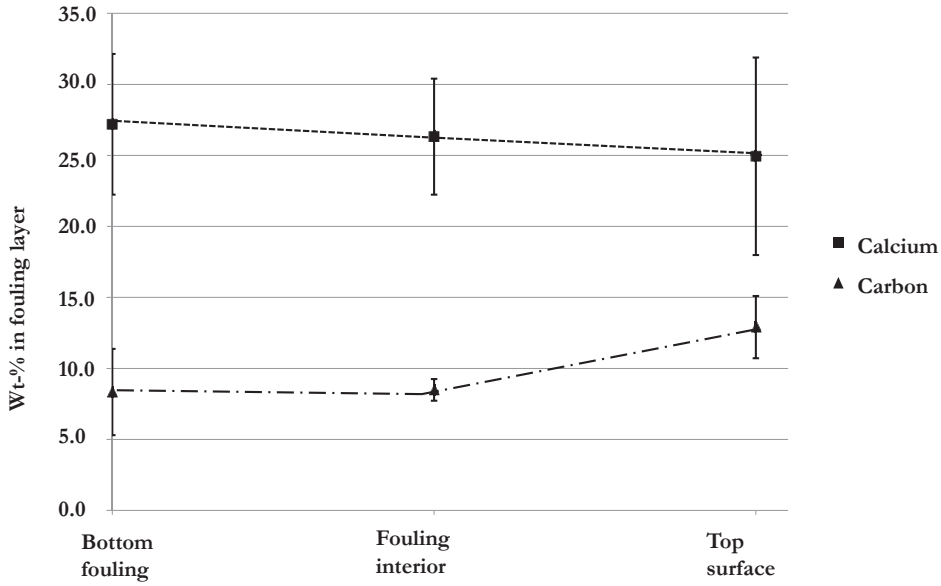

Figure 9 The results of the EDX measurements categorized according to the three subsections of the fouling layer: the first 50 µm closest to the metal surface; the interior of the fouling layer; and the outermost part of the fouling surface, towards the fluid. The top line (- -) indicates the calcium concentration and the bottom line (- .-) indicates the carbon content.

The carbon content of the fouling seems to be somewhat higher towards the bulk, as evidenced from the EDX analysis. This concords with the presence of smooth areas, as indicated by an arrow in Figure 6A and shown at higher magnification in Figure 10. The smooth areas shown in Figure 10 contain 25% carbon, as compared to the rough structure in other areas in the fouling, which contains only approximately 8% carbon. The smooth areas do not completely cover the upper surface of the fouling layer but are instead detected as islands on the surface.

The smooth areas are not found elsewhere in the fouling layer, only on the top, closest to the product flow. One theory to explain their origin is that the clusters are aggregates of whey protein that attach to the top of the fouling but are not firmly incorporated into the rest of the structure. In that case, they should be easily removable by the flow and not be found further down in the structure. It could of course also be the case that these smooth structures are incorporated and hidden in the mineral-rich structure as it grows. The high-magnification CLSM images may

support the idea that the protein layer to some extent encapsulates the mineral domains throughout the fouling layer.

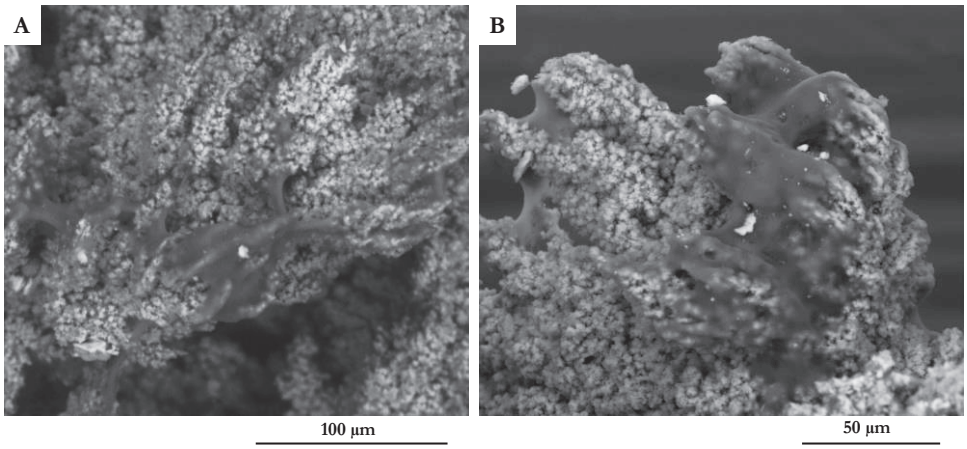

Figure 10 Smooth areas on the fouling surface contain high concentrations of carbon, as seen in A, which is an image taken from the top of the fouling surface, and in B, which is a higher-magnification image taken from the side of the sample.

3.3.3 Wide Angle X-ray Diffraction (WAXD)

WAXD is a structure analysis technique that has been used to study the crystallinity of the calcium phosphate in the fouling layer. The investigation of the structure of the calcium phosphate component of the UHT fouling is of interest for determining whether the mineral has the amorphous form seen in casein micelle nanoclusters or if the mineral forms a crystalline structure within the layer. Highly ordered apatite structures have been reported previously to occur at high temperatures [9, 14, 39, 64, 65], so a crystalline structure was expected. The result of a WAXD analysis is commonly presented as the intensity of the diffracted x-rays, either as a function of diffraction angles, 2θ, or the momentum transfer, Q ($Å^{-1}$):

$$Q = (4\pi \sin(\theta/2))/\lambda \quad (3.1)$$

where θ (°) is the angle of incidence and λ (nm) is the wavelength. Figure 11 shows the diffraction for the UHT fouling recorded in the Q-range between 0.11 and 2.89 $Å^{-1}$.

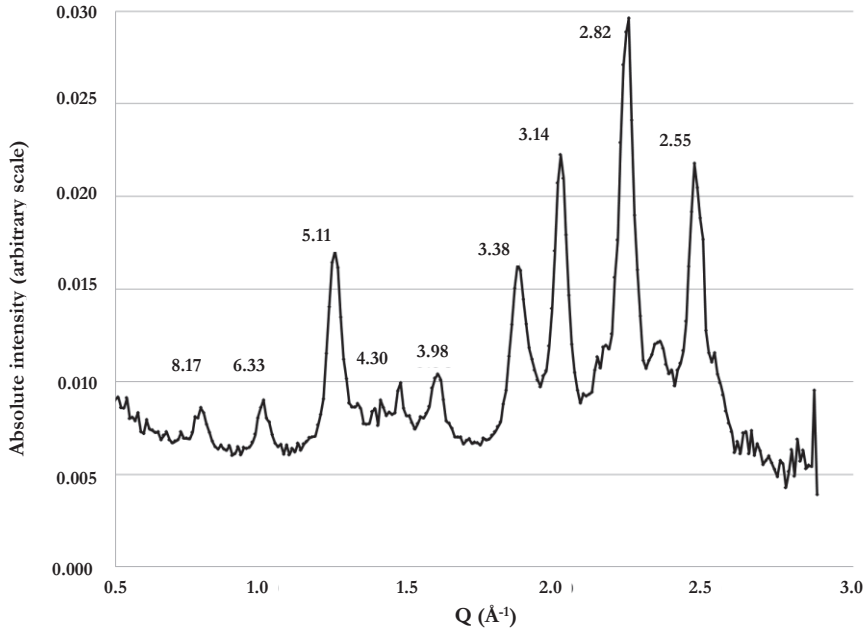

Figure 11 Crystallographic analysis revealing a crystaline mineral structure with clear resemblance to β-$Ca_3(PO_4)_2$. The data indicated at each peak are the Bragg reflection spacings, d.

The values correlated to the peaks in the diffractogram, ranging from 2.55 to 8.17, are the Bragg reflection spacings (Equation 3.2), and they have, with comparisons to data in the literature, been used to reveal the structures of the calcium phosphates [64].

$$d = 2\pi/Q \tag{3.2}$$

The diffractogram from wide angle x-ray scatter analysis shows a crystalline structure for the calcium phosphate matrix, corresponding to a distorted lattice of β-$Ca_3(PO_4)_2$. This structure has been observed in previous studies looking at the changes in calcium phosphate structure upon heating, and it is similar to the apatite structure found in bio-minerals [17, 39, 64, 65].

Summary

The structure and composition of UHT fouling have been thoroughly investigated in different length scales. The fouling has been confirmed to have a high mineral content, as postulated in the late 1960's by Burton [14]. The high-temperature fouling examined in the present study comprises approximately 70% calcium phosphate and 10% protein. The composition is evenly distributed throughout the structure and does not show any significant spatial variation in the direction perpendicular to the surface.

The fouling is constructed from spherical structures that contain both proteins and minerals, and the mineral part has a clear crystalline structure that is likely due to the high temperature used for UHT processing. The fouling structure grows outwards from the stainless steel surface and is clearly affected by the flow pattern during processing. Aggregates of proteins and minerals are possibly formed in a bulk reaction, which is then connected to the growing fouling layer through an adhesion process.

The flow helps to create pillars of fouling, thereby generating a heterogeneous structure with deep valleys and high mountains. This rough structure is likely to have an impact on the cleaning process, since it creates the area that comes in contact with the cleaning solution. The implications of this are discussed further in Chapter 5.

4 Production of UHT milk fouling

UHT fouling is usually formed in aseptic process lines and is therefore difficult to study *in situ*, since it is difficult to remove it from the process equipment for investigation. To study this high-temperature fouling, pilot equipment has been used to produce fouling that has the relevant characteristics and that can be removed from the production unit. This chapter is based on the information and data reported mainly in Paper I.

4.1 Pilot-scale production plant

One of the first issues in this project was to create an experimental fouling system that is relevant to the phenomena we want to study. The production of UHT fouling under controlled conditions that provided samples with the same properties as the fouling found in industry was the main goal in designing the pilot-scale production plant.

For this purpose, long production runs with skim milk are needed. It has been shown that it is of importance for fouling layer build-up that the milk passes only once. Recirculation would carry the risk of removal of the fouling components from the solution and this would not give an accurate representation of the industrial fouling layer. It was therefore important that the equipment was designed in such a way that it was possible to connect it to a process stream in a dairy.

The pilot plant used processes skim milk for 15 hours at a flow rate of 500 L/h, which corresponds to a flow velocity of 0.85 m/s through a pipe with a diameter of 14.4 mm. The flow is a fully developed turbulent flow with Reynolds number, Re= 46,300. The Reynold number is given by:

$$Re = v * L * \rho / \mu \qquad (4.1)$$

where v is the velocity (m/s), L is the length or in this case the hydraulic diameter (m) of the pipe, ρ is the density (kg/m^3), and μ is the dynamic viscosity (kg/m*s) of the fluid. The Reynolds number gives information regarding the relationship between the inertial forces and the viscous forces of the liquid. When the viscous forces are less than the inertia of the liquid a turbulent flow pattern is achieved.

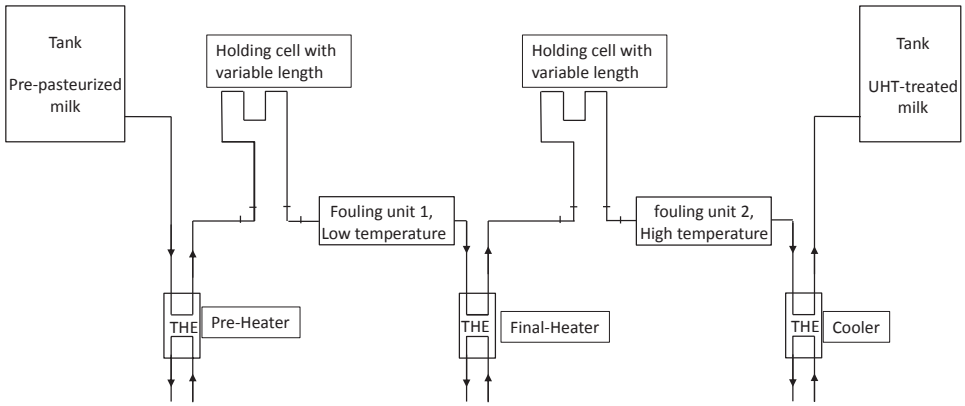

Figure 12 Schematic figure of the pilot plant fouling equipment. The two fouling units (1 and 2) can easily be altered to change the process time and temperature by changing the number of tubes in the pre-heater, final heater and/or the two holding cells, respectively.

A schematic of the pilot plant used to produce the fouling is shown in Figure 12. The produced fouling is collected at two separate fouling units. The first fouling unit is located after the preheating section in the pilot plant, and this fouling has the characteristics of a low-temperature or type A fouling (Table 1, Chapter 3.3). As mentioned earlier, the preheating section is used to pre-denature the protein before the section with the final heater, which accounts for the lower rate of fouling in that section [14]. The temperature of the preheating fouling unit was not regulated separately but was maintained at approximately 100°C.

The fouling formed in the UHT section of the pilot plant was located after the final heater but before the cooling section. The temperature of the UHT section was 137°C and was kept constant for the entire period of production. The holding cell for the UHT treatment retained the milk for 8 seconds. The time-temperature characteristics of the production plant are shown in Figure 13. The differences in the visual appearances of the fouling layers formed at different temperatures are shown in Figure 3 (Chapter 3.1), whereby the protein-rich, low-temperature

fouling has a more translucent appearance than the mineral-rich, high-temperature fouling.

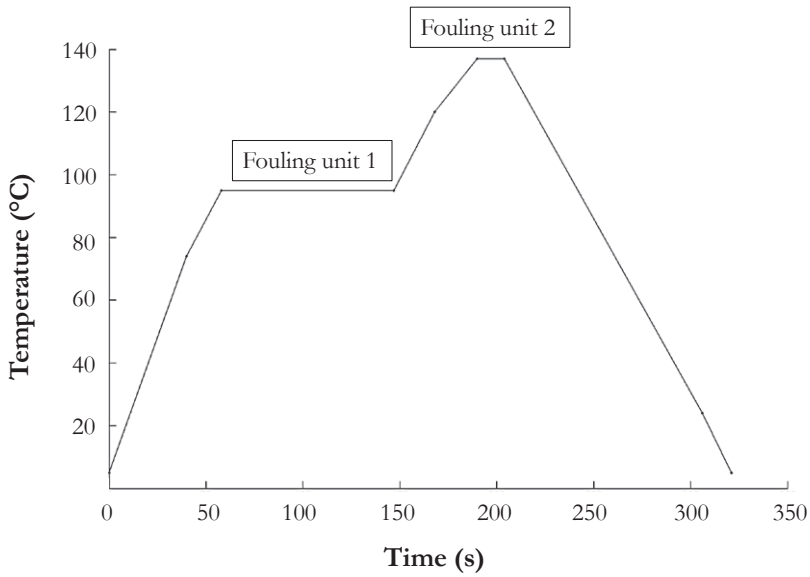

Figure 13 The time-temperature curve used for the design of the fouling pilot plant used to generate both low-temperature fouling (in Fouling Unit 1) and high-temperature fouling (in Fouling Unit 2).

The two fouling units were built to hold stainless steel coupons that could be removed from the production plant. The fouling units each contain 20 stainless steel coupons that face each other from the side of the rectangular-shaped fouling unit. From the beginning, the coupons were designed to have a flat surface facing the product flow with an area of 40×16 mm.

During the design of the pilot plant, several online techniques for measuring the fouling layer thickness during cleaning were considered. The cleaning unit has a window for visual inspection and for thickness analysis by laser triangulation, which requires that the production pipe has a flat surface rather than a regular tubular shape. The removable fouling unit is therefore built in a rectangular shape, but having flow patterns similar to those for the tubular shape found in the rest of the heat exchanger. The flow velocity in the fouling units was 0.83 m/s, which is in the turbulent regime with Reynolds number, Re = 40,500.

The run time for the production unit was calibrated for processing times of between 8 and 24 hours. For 8 hours, the fouling layer was found to be thin and difficult to measure with the laser triangulation sensor chosen as the primary online analysis tool for the cleaning studies. Using a 24-hour run time produced such a thick fouling layer that the equipment became blocked before reaching the desired production time. To create reproducible fouling of sufficient thickness, a run time of 15 hours was chosen for the trials designed to analyze the structures and the cleaning parameters. The thickness of the fouling layer varied between approximately 100 µm and 500 µm due to the flow pattern in the section. Fouling thickness was followed in the regions of the thinner layer, whereas the structural analysis was performed on the thicker pieces of fouling. The UHT fouling was brittle and the thicker pieces were used for the offline analysis to minimize the risk of destroying the sample during sample preparation.

4.2 Coupon optimization

When the production time was calibrated a somewhat unexpected result was obtained. The rectangular shape of the fouling unit had a drawback. A fouling with even roughness was formed on the flat surface, although the physical tension within the structure attributed to the rectangular shape caused the fouling layer to detach from the surface when the unit was disassembled (Figure 14).

Figure 14 Image showing how the UHT fouling layer detaches from the metal surface during dissassembly of the fouling unit when the geometry of the fouling coupon is not optimized.

To be able to study the cleaning effects on UHT fouling, the fouling must be attached to the stainless steel surface. Several coupon geometries were tested to derive a fouling layer that adhered as strongly to the surface as in the tubular section of ordinary regular UHT production plant.

In the tubular sections at the end of each rectangular pipe, the fouling was firmly attached and could not be easily detached from the surface. The tubular shape is thought to exert an impact on surface attachment, and the final optimization of the coupon shape was to mimic a semicircle and leave room for visual online inspection during cleaning. The semi-circular coupon features a ledge at the top (Figure 15), which prevents the fouling layer from detaching when the coupon is removed from the production unit.

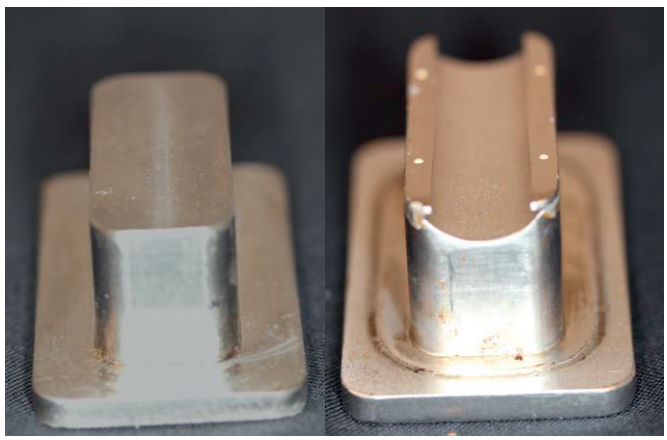

Figure 15 Images of the coupons used in the fouling formationunits. To the left is the original coupon with a flat surface facing towards the product flow, and to the right is the final optimized semi-circular coupon top with a ledge.

It should be noted that this alteration of the coupon produces a disturbance in the flow pattern where the coupon is indented to form a semi-tubular shape. During the cleaning studies, care was taken to have the flow of cleaning solution in the same direction as that used for the production process, so as to minimize the impact of this flow disturbance, as discussed in Paper III.

Summary

The fouling equipment, which was designed, produced, and optimized in this study, has been used to mimic successfully UHT fouling in an industrial setting, using industrially relevant parameters. Therefore, this fouling was expected to

have the same composition as the fouling found in industry. Another issue that has been resolved is the need to study the changes that occur in the fouling layer online during cleaning. A system that collects fouling on coupons, which can thereafter be transferred to a separate cleaning unit, has been established. An important aspect of the coupons is their geometry; a semi-circular coupon allows for fouling build-up without the built-in tension that would otherwise detach the fouling from the surface. The problems related to equipment geometry, which can lead to detachment of the fouling from the surfaces, faced in this project could of course be regarded as beneficial if firm attachment of fouling is not desired.

5 Cleaning of UHT milk fouling

The design of an optimal cleaning process requires knowledge of the deposit structure and composition, as well as of the mechanisms that control the cleaning process. The main goal of this project has been to obtain a mechanistic understanding of the process of removal of the fouling that is produced during UHT treatment based on acquired knowledge of the fouling layer structure and composition. It is of importance to understand how different cleaning parameters affect the cleaning efficiency. The results discussed in this chapter are mainly based on those presented in Papers III and IV.

5.1 Removal of fouling from heated surfaces

5.1.1 Fundamentals of cleaning

The development of an efficient cleaning process for the food industry is challenging in the sense that there are different definitions of the concept of cleanliness. Cleanliness can mean bacteriologically clean or sterile or it can also refer to a chemically or physically cleaned surface [3]. In this project, the concept of cleanliness refers to surfaces that are physically and chemically cleaned, i.e., the removal from the equipment surface of fouling materials derived from the proteins and minerals in the milk, in order to restore the original surface properties of the material.

UHT milk fouling is commonly removed using a closed cleaning-in-place (CIP, Table 3) system with a two-step cleaning process that employs an alkaline detergent, usually one based on NaOH, to remove the organic components of the fouling, followed by an acidic detergent, usually nitric acid, to remove the mineral components.

Process step	Cleaning agent	Concentration	Temperature	Time
Water rinse			Hot	10 min
Alkali cleaning	NaOH	0.5–1.5 wt%	75°C	30 min
Water rinse			hot	5 min
Acid cleaning	HNO3	0.5-1.0 wt%	70°C	20 min
Water rinse			cold	

Table 3 Examples of cleaning processes for pasteurization equipment. The rule of thumb in industry is to clean the equipment at the production temperature. The UHT equipment also needs to be sterilized to ensure that the equipment is bacteriologically clean [3].

Sometimes the alkali cleaning solution contains surfactants, which are surface-active agents that contain one hydrophilic part and one hydrophobic part. The surfactants are added to increase the wettability of the surface, facilitate the removal of the fouling, and aid in dispersing any fat that might be captured in the fouling layer. As surfactant performance tends to be sensitive to temperature changes, formulated cleaning solutions have a maximum/optimum cleaning temperature. For UHT fouling, this could be problematic, since the role of thumb in industry is that alkali cleaning should be performed at production temperatures, which might not coincide with the optimum temperature surfactant action [3]. Sequestering agents are also used in formulated cleaning solutions to complex with ions from the fouling, thereby increasing the efficiency of the subsequent acid cleaning step, but also to prevent the formation of (insoluble) complexes between the surfactant and, in particular, multivalent ions.

In this project, since the focus has been on understanding the mechanisms associated with alkali cleaning, the alkali cleaning solution used did not contain surfactants or sequestering agents; only a pure NaOH cleaning solution was used. Four parameters are considered crucial for the efficient removal of fouling from surfaces:

- Temperature
- Flow velocity
- Detergent concentration
- Time

It is common practice that the alkali cleaning is performed at the same temperature as the production and that the acid cleaning temperature is set at approximately 75°C. The flow velocity gained from the industrially designed cleaning circuits usually lies between 1.5 and 3 m/s.

CIP cleaning with two cleaning steps, alkali and acid, is performed for 20–60 minutes, depending of the product that has been processed. The concentration of NaOH used is between 0.5% and 1.5%, but as we will see the optimal concentration is dependent upon the fouling structure and composition. For an acid solution, the corrosive effect on the stainless steel needs to be take into account, and the recommended dosage of HNO_3 is between 0.5% and 1% [3].

The cleaning process can be considered as having three stages: 1) the cleaning agent is transported, through a combination of convective mass transfer and diffusion, to the fouling layer where it penetrates the fouling; 2) a chemical reaction occurs that changes the structure of the fouling; and 3) the fouling layer is removed from the stainless steel surface, either through the diffusion of smaller molecules or through mass transfer of larger pieces.

An alkali cleaning agent is considered to react primarily with the organic material in the fouling, whereas an acidic cleaning agent reacts mainly with the mineral part of the fouling. Acidic cleaning solutions can however cause a protein-rich fouling to form an acid-induced gel [66] that might hamper the cleaning process. Knowledge of the fouling layer structure and composition, as well as the efficiency of the alkali cleaning step can therefore be crucial for improving the overall cleaning efficiency [67]. The spatial distributions of minerals and proteins, as well as the porosity and the thickness of the fouling layer can influence the

penetration of the cleaning agent and the subsequent dissolution/degradation and removal of the deposits.

Properties of the fouling, such as cohesive and adhesive strengths, have previously been shown to vary with the composition of the product. Cohesion refers to the forces that hold the internal structure together, whereas adhesion is the force that keeps the structure attached to another material, in this case the stainless steel of the process equipment. There is no straightforward answer as to which of these forces is the strongest in a fouling layer. For example, in tomato paste, the cohesive strength is greater, whereas in the milk protein fouling produced from whey protein concentrate (WPC), the strength of adhesion to the bottom surface is greater [68, 69]. At least for low-temperature fouling with high protein content, these properties are crucial for determining if the fouling will be dissolved from the top down or if the fouling can be detached in lumps by the flow [70, 71].

In the acidic environment of the second cleaning step during CIP, the mineral fouling layer is removed; studies have been conducted to examine the mechanisms for removal of the mineral layer [72]. The removal of calcium phosphate depends on the crystalline structure of the deposit, where dissolution of the structure is considered to be faster than mass transfer from the fouling layer. For a mixture of dicalcium phosphate dehydrate (DCPD) and hydroxyapatite (HAP), the limiting factor during cleaning in a turbulent flow is the mass transfer of dissolved particles from the surface. When DCPD is the sole foulant, the deposit is removed in lumps by the shear force of the fluid flow [72]. The process of dissolution of the mineral fraction has not been studied in detail in the present work, but as will be shown in Figure 24, the mineral deposit is eroded layer by layer, indicating a mass transfer-limited mechanism for the removal.

The transport of the active agent in a cleaning solution to the fouling surface and its penetration through the fouling layer connects two phenomena: convective mass transfer and molecular diffusion. The molecular flux, N_A (mol/m^2*s), of active molecule A in the cleaning solution during convective mass transfer can be generalized in the form:

$$N_A = k_c * \Delta c_A \qquad (5.1)$$

where k_c is the convective mass transfer coefficient, and the flux is dependent upon the concentration gradient between the bulk and the area close to the surface. The Sherwood number (Sh) can be used to describe this phenomenon under forced convection in a tubular-shaped unit, and it is a function of the Schmidt number

(Sc) and the Reynold number (Re). For turbulent flow in a pipe, the Sherwood number can be written as:

$$Sh = .026 * Re^{0.8} * Sc^{0.33} \quad (5.2)$$

Sh defines the ratio between the rate of (convective) mass transfer and the rate of diffusion and Sc represents the relationship between the viscous diffusion (dynamic viscosity) and mass diffusion rates. The Reynold number gives, as presented in Chapter 4.1, the relationship between the inertial forces and the viscous forces of the solution.

$$Sh = k_c/(\frac{D}{L}) \quad (5.3)$$

where D is the diffusion coefficient (m^2/s) and L the length of transfer (m).

$$Sc = \mu/(\rho * D) \quad (5.4)$$

where μ is the dynamic viscosity of the cleaning solution (kg/m*s) and ρ is the density (kg/m^3). Molecular diffusion within the fouling layer can be described as the net flux (J) of cleaning agent due to a concentration gradient into the fouling layer [43], and this can be described by Fick's first law of diffusion (5.3).

$$J = D * dc/dz \quad (5.5)$$

The diffusion coefficient, D, (m^2/s) can either be determined experimentally or estimated based on the size of the molecule, derived from the Stoke-Einstein equation. The diffusion of the cleaning solution is regarded as a rapid process. The molecular diffusion of hydroxyl ions in water is given by [73]:

$$D_{OH} = 6.64 * 10^{-7} * e^{-E_a/RT} \quad (5.6)$$

For the UHT fouling studied in this project, there is an extensive mineral network that will act as an obstacle to diffusion. The porosity has been shown to be approximately 50% of the fouling layer in which the cleaning agent can freely diffuse and the diffusion coefficient is therefore regarded as being half of the value of the free diffusion, D_{OH}.

In addition to the transport of cleaning agent, diffusion of dissolved compounds through the fouling and the boundary layer occurs in the opposite direction, removing the fouling from the surface. For the protein network, this includes not only diffusion, but also the disentangling of the separate protein molecules. The convective mass transfer discussed earlier is of course also involved in the removal of the fouling layer.

Between the transfer of hydroxyl ions into the fouling layer and the transfer of fouling material out from the layer, a chemical reaction occurs. The hydroxyl ions react with the organic compounds, mainly the proteins in the fouling. For most of the available cleaning models, this can be described as a first-order reaction:

$$k_r = c_{OH} * e^{E_a/RT} \quad (5.7)$$

Low-temperature, protein-rich fouling removal has been studied extensively and several models for the removal mechanisms have been presented [68, 70, 74-76]. The gels observed during studies of milk fouling are usually formed at temperatures of <100°C and mainly consist of protein. For pure β-LG, the gel will be stranded and therefore transparent, whereas for mixtures of several types of whey proteins, a particulate structure and an opaque gel will be formed [34]. The stranded and particulate gels from whey protein have different properties, and the particulate gel is more relevant for cleaning studies that aim to mimic the natural behavior of low-temperature milk fouling [77]. Therefore, the model systems tend to be based on WPC or whey protein isolates (WPI).

Cleaning processes for protein-rich gels have been described using a model of polymer dissolution [70]. This model has three main stages, as do several other models [47, 77, 78] (Figure 16). The first stage is a swelling/reaction stage, which is followed by a uniform removal stage during which most of the fouling is removed, and then a final stage with a decaying rate of removal. Swelling is usually considered to be the result of a combination of chemical and physical reactions [70, 76, 78-80].

The most important result obtained from the model developed by Xin et al. [70] was the constant cleaning rate during the swelling/reaction stage, and this was used to estimate the amount of removed fouling during alkali cleaning. The rate-limiting step in that study was considered to be the removal of the disentangled proteins away from the fouling layer, although this has been challenged in studies of the dissolution process of β-LG, which have shown that the dissolution of protein gels formed at higher temperatures requires a high activation energy (due to of the presence of disulfide covalent bonds). Thus, the dissolution reaction is slower and so the mass transfer cannot be considered to be the only rate-limiting step [81].

During the removal stage, the protein-rich fouling is considered to be removed in patches in a first-order reaction [47, 70]. This behavior is not observed for the mineral-rich fouling studied here, whereby the rigid mineral network protects the protein network (Paper IV).

The efficiency of dissolution of protein from the gel is thought to be dependent upon the swelling of the protein network. If the swelling is inhibited, the dissolution or cleaning is supposedly less efficient. This implies that here is an optimal cleaning concentration of NaOH, and this has been defined as 0.5 wt% [47, 78, 79, 82]. When the concentration of alkali is too high, a gel-like layer is produced on the surface, which prevents the transport of the degraded protein units out into the bulk solution [47, 75, 83]. For UHT fouling that has a low concentration of protein, this phenomenon is not observed, so the rate of cleaning is increased with a higher concentration of cleaning agent? (see Chapter 5.4).

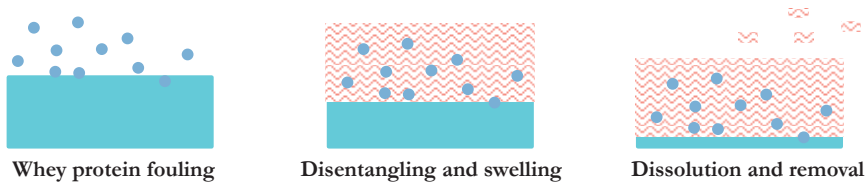

Figure 16 Schematic explaining the whey protein cleaning process. The blue solid layer is the fouling before cleaning and the red stripes depict the swelling protein layer. The hydroxyl ions are shown as blue dots in the images. During whey protein cleaning, the network swells dramatically and is removed from the surface as the nework is disentangled and degraded. High concentrations of alkali decrease the rate of removal by forming a gel-like structure at the top, which hinders the swelling and dissolution of the proteins.

The dissolution of the protein network in an alkali solution is partially due to β-elimination of the disulfide bridges formed during heat treatment. The activation energy (E_a) for the breaking of this covalent bond by an alkali cleaning solution is around 76 kJ/mol [81]. The reaction at a relatively low concentration of alkali is suggested to be slow, releasing larger complexes of protein to disentangle from the network, decreasing also the mass transfer from the surface of the gel layer [81]

Whey proteins are commonly found in low-temperature fouling, whereas caseins are thought to be more predominant in high-temperature fouling [28]. Casein fouling has generally not been regarded in the models developed for fouling or cleaning. These models attempt to explain either the low-temperature fouling zones or the mineral part of the deposit in the high-temperature zones.

The mineral deposit present in high-protein fouling is thought to be transferred into the bulk together with the protein during alkali cleaning [75] or through a dissolution process during the acid cleaning step. The rationale for using an acidic

cleaning solution is to dissolve the mineral deposits by lowering the pH. Calcium phosphate needs a low pH to dissolve the formed crystals according to the scheme below:

$$2\,H^+ + Ca_3(PO_4)_2(s) \rightleftarrows 2\,H(PO_4)^{2-} + 3\,Ca^{2+}$$

Dissolution, together with the action of shear forces from the flow, is of importance for the removal of mineral deposits [84]. A cleaning model that is adapted to fouling that is rich in minerals and that has a low but significant concentration of protein has not been presented to date. The mechanism for cleaning of the predominant mineral-based, high-temperature fouling cannot solely be explained by evaluating and understanding the removal of a mineral or a protein layer; a combination of the two types of deposits has to be considered. In Chapter 5.5, a first model for the mechanisms of cleaning UHT fouling is presented.

5.2 Pilot-scale cleaning unit

Studying the cleaning and removal of high-temperature fouling is complicated due to its high mineral content, which is not easy to reproduce using a model system. The few studies of high-temperature fouling have been performed on a larger scale, such as this project and that for recirculating milk [5, 12, 16, 85]. The pilot-scale fouling unit that was built within this project is presented in Chapter 4, and in this chapter, the separate pilot-scale cleaning unit (Figure 17) is described. The equipment is designed to allow the performance of cleaning experiments according to protocols that are industrially relevant, using stainless steel coupons with fouling that are produced in the fouling production plant.

The cleaning parameters that have been investigated in the project are all well controlled in the cleaning pilot plant. The solution of cleaning agent is dosed in the balance tank and the detergent concentration is regularly and carefully controlled with good reproducibility using pH titration.

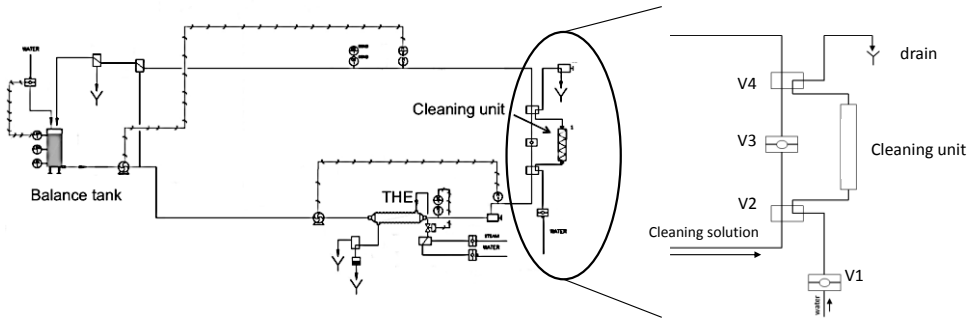

Figure 17 Schematic of the pilot plant cleaning set-up used for ***in situ*** studies of fouling removal. The tubular heat exchanger is marked as THE. V1 to V4 mark the valves used to control the flow through the cleaning unit.

The equipment contains two separate loops: a larger one where the parameters can be adjusted before reaching the fouling, and a smaller loop called the 'cleaning unit' (Figure 17), where the fouled coupon is located. The solution is pumped into the big loop of the equipment, not passing the fouling in the cleaning unit, until the right velocity and temperature are reached. The equipment is run at an elevated pressure so as to reach a cleaning temperature that is appropriate for the removal of UHT fouling.

When the parameters of the cleaning solution are correct, the V2, V3 and V4 valves (Figure 17) are opened so that the solution can pass over the fouling layer situated in the cleaning unit. The cleaning unit consists of a rectangular channel with the same dimensions as the rectangular channels used for fouling production. The cleaning unit supports one or (at a maximum) two coupons for simultaneous cleaning and contains windows for the use of analytic instruments (see Figure 5 in Paper I). The cleaning unit is also connected to a separate cold water feed that is used to rinse the system separately so that the chemical reactions between the cleaning solution and the fouling layer can be quenched and the exposure time for the detergent can be accurately controlled.

The pilot plant is designed so that the period of time during which the fouling comes in contact with the cleaning solution can be accurately controlled, as well as the temperature and concentration of the cleaning solution. The use of coupons in the cleaning unit is beneficial for the reproducibility. Many coupons are used to produce fouling in each batch of fouling, which means that the fouling is from the

same batch and has experienced the same conditions, and that the risk of individual differences in fouling properties is reduced.

A two-step cleaning process is used throughout the project, and the parameters investigated are systematically changed from one standard reference protocol. The reference cleaning protocol involves a two-step cleaning process in which the first cleaning agent is 1.5 wt% NaOH, used at 100°C and at a flow velocity of 1.6 m/s. During the study of the impacts of the parameters and the investigations of compositional and structural changes, the protocol for the first alkali step was changed (Table 4).

Parameter	Referemce value	Increased value
Temperature (°C)	100	120
Fluid velocity (m/s)	1.6	3
Alkali concentration (wt%)	1.5	3

Table 4 List of parameters that are varied in this work. The parameters are applied for a wide range of processing times, from 1 min to 30 min.

The second step in the cleaning protocol, the acid cleaning, was not changed during this project. The cleaning was maintained using 0.5 wt% HNO_3 at 80°C and at a flow velocity of 1.6 m/s. As acid cleaning is a rapid process, to have sufficient time to record the impact of the previous alkali treatment, the acid concentration was not altered. In industry, the general recommendation when nitric acid is to be used for CIP is to use a concentration of 0.5 wt% to 1 wt% at a temperature of 75°C [3].

5.3 Measurement techniques

The analyses of the removal and of the structure and composition of the fouling during the cleaning process are an important part of this work. Different cleaning protocols were used in order to understand the impacts of the different steps of the process, which were monitored both online during cleaning, as well as offline by pausing the cleaning to take snapshots of the structure and composition of the fouling during the cleaning process.

5.3.1 Online analysis

The online process of cleaning was studied visually with a Canon EOS 600 a camera, fitted with an EF-S 60/2.8 macro objective that takes macroscopic images with short time intervals. To be able to control the light setting for the camera, a ring-formed flash was used (Canon MR-14EX II). To follow the sequence of the cleaning behavior during alkali cleaning, images were collected every 20 seconds. The cleaning process during the acid cleaning is faster, so the images were recorded every 10 seconds.

The camera was useful for visualizing the difference between an efficient and an inefficient cleaning process. The concept of efficiency is defined in this project as a situation in which the acid cleaning allows for the mineral network to be removed and leaves a clean surface without residues. This definition is further discussed in Chapter 5.4.

Using a window inserted into the cleaning unit, the thickness changes of the fouling layer during cleaning could be followed. The thickness was measured with a laser triangulation sensor (optoNCDT 1700-10; Micro-Epsilon, Ortenburg, Germany). This sensor works by emitting a beam from the light source perpendicular to the surface. When the light hits the surface it is scattered and reflected, and this light is collected. The angle of scatter can then be correlated directly to the distance between the sensor and the surface.

The sensor is highly sensitive to changes in refractive index. Given its high sensitivity to small changes in temperature, it is challenging to determine the correct value of the thickness. To avoid incorrect measurements due to temperature fluctuations, the thickness measurements were reduced to a three-point analysis (Figure 18). In Paper I, the concept for thickness measurement with

the laser triangulation sensor was not fully optimized and is therefore not corrected for the temperature changes in the system. In Paper I swelling is seen to occur in the fouling layer, but due to the temperature fluctuations in the beginning of the cleaning run, the cause of this thickness increase cannot be accurately determined.

The thickness measurements were performed with rinsing with cold water at the same temperature before and after the cleaning process, to establish the original height of the fouling layer. During the water rinse step between the alkali and acid cleaning steps, an intermediate point was taken to visualize the change in thickness during the first alkali cleaning step.

Another correction for the refractive index of the medium was made. The correction factor was determined by measuring nine points with a known distance to the metal surface from the sensor, both in air and in cold water. The ratio for air/water for a known distance is regarded as the correction factor and calculated as F=1.53. The end-point of the acid cleaning step is defined as the point at which a clean metal surface is visible at the position of the laser. This time-point was defined with the help of a video camera.

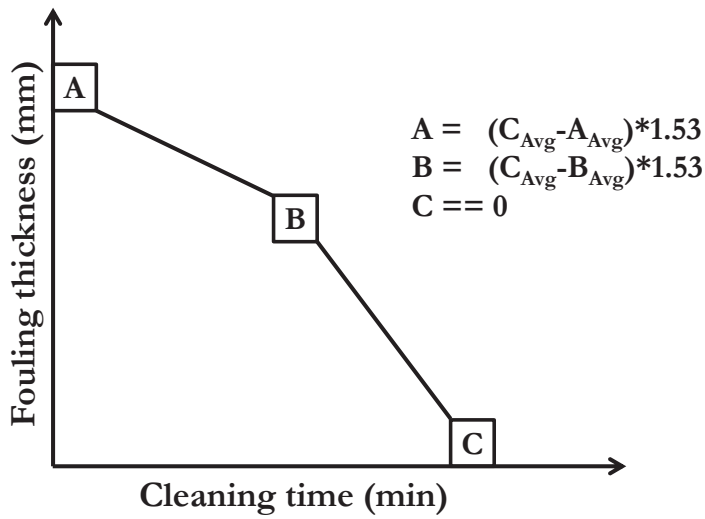

Figure 18 Three-point analysis of the thickness of the fouling, as measured in cold water before and after the cleaning, as well as between the alkaline and acid cleaning steps. Points A, B and C are measured in water in a narrow temperature interval. The average of these values is used together with the correction factor F = 1.53 to visualize the overall effect of the different cleaning stages.

The fouling layer showed some interesting features with regards to changes in thickness. Proteins in an alkali environment are known to react by swelling due to the breaking of disulfide bonds (if present) and due to increased electrostatic repulsion between the protein molecules in the network [78]. Instead, the UHT fouling layer thickness in this work decreased during alkali cleaning. The thickness decreases by 40%±20%, as shown in the top graph in Figure 19

If the proteins swell in the fouling network, the network might also collapse in the cold water rinse. The fouling layer has high-level porosity within the structure and the protein network would also be able to swell within the structure without this being visible from the top surface or being detected by the laser triangulation sensor. Patches of high protein content are detected on top of the fouling layer, which are not visible to the naked eye (Figure 10). These patches disappear early on in the alkali cleaning (Figure 20), and are presumably removed in the same manner as a regular protein gel. If these patches are captured by the laser beam spot, some of the reduced thickness could be explained, but not the extent recorded by the laser.

The result obtained from the laser sensor is a puzzling aspect of this project, since the large drop in fouling thickness was not verified by the structural analysis. One explanation for the decrease in fouling thickness could be the decrease in surface density with duration of cleaning. Images illustrating the decreased density with time are shown at the bottom of Figure 19, which also presents images of fouling layers that have been cleaned with alkali for 1 minute (left) and 16 minutes (right), both with the standard protocol. Already after 1 minute of cleaning, the number of patches with high protein content has decreased at the surface, and after 16 minutes, a slightly lower relative amount of organic carbon is expected (Figure 20).

The red circle in Figure 19 illustrates the size (minimum 50 μm) of the laser spot used in the laser sensor for thickness measurements. At a low magnification, the structure may appear not to have changed during cleaning. However, at higher magnification, it becomes obvious that the fouling layer has been altered and that the laser sensor is likely to be affected. The laser sensor uses the diffuse reflective light from the beam as it is reflected onto the surface, and with cleaning the intensity of the reflected light is likely to have decreased and changed.

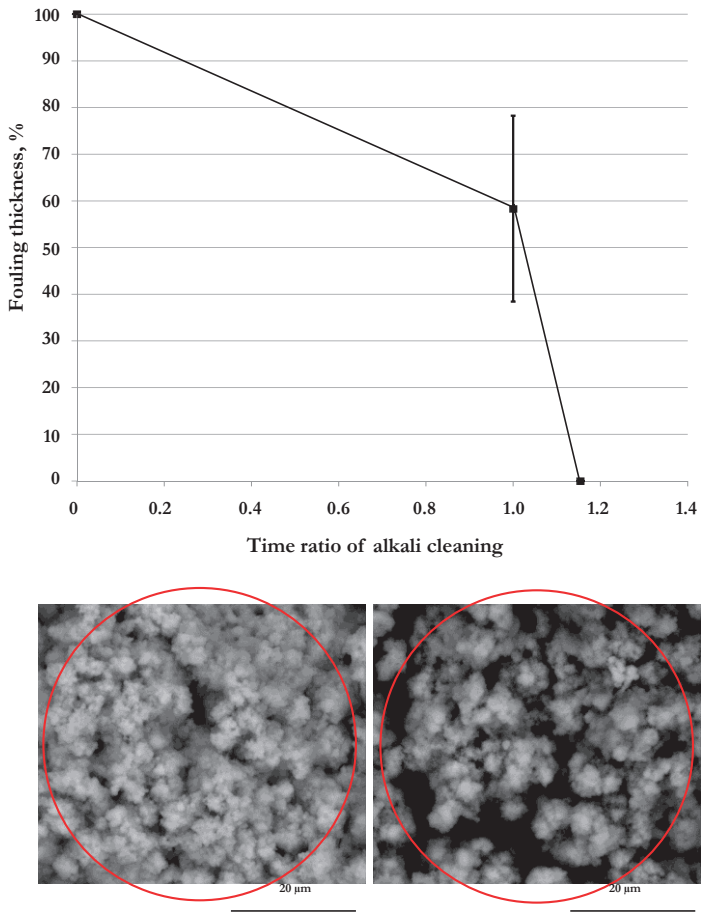

Figure 19 Top graph shows the change in fouling thickness during the first cleaning step (alkali) followed by the second (acid) cleaning step. The bottom images show the structure viewed from the top of the fouling after 1 min and 16 min of alkali cleaning, respectively. The conditions for both cleaning times were 1.5% NaOH at 100°C and flow rate of 1.6 m/s.

It is important to point out that the data shown in the upper graph in Figure 19 originate from data obtained from studying the effects of different cleaning parameters (Paper III), and are characterized as representing efficient cleaning protocols. Therefore, the graph does not include thickness changes for inefficient removal of the fouling layer. The parameter times found in the efficient cleaning regime are presented in Figure 25.

5.3.2 *Offline analysis*

The offline analysis gives additional and more detailed information regarding the changes that occur during cleaning. The methodology of the offline analysis used in this project has been discussed previously (Chapter 3). SEM, CLSM and EDX were used to reveal the fouling structures and compositions at different stages of cleaning. The observed effects of the cleaning process on the fouling layer have here been divided into structural and compositional changes. The main phenomena analyzed in this project are the effects of the reactions that occur between the fouling and the alkali cleaning solution, that is, with the protein part of the interconnected network. Since the major part of the fouling consists of a rigid mineral network, no visible changes in structure due to chemical reactions with the proteins were expected.

Compositional changes in UHT fouling during cleaning

The composition of the fouling and the spatial variation were investigated in this project, and the results from the EDX and chemical analyses gave consistent results. In the cleaning studies, the amount of fouling left after cleaning was not sufficient to allow for chemical analyses at the different levels of cleaning. The composition of the fouling after the cleaning process was therefore assessed with EDX only. The cleaning efficiency with regard to the chemical composition was assessed by analyzing the amount of carbon. Carbon is a good indicator of the amounts of organic compounds in the fouling layer and is relevant to study during alkali cleaning since the cleaning solution mostly affects the protein part of the network.

The most significant change in the concentration of carbon is seen at the top surface (Figure 20). The patches of protein disappear quickly. With the reference cleaning protocol, these patches can be found after 1 minute of cleaning, whereas at an elevated temperature, the change happens before the first minute has elapsed. Over time, as the cleaning proceeds, a decrease in the levels of carbon compounds, e.g., proteins, is noticeable. This decrease is however small, and the error bars are relatively large, so no firm conclusions can be made. The trend of only a small variation in carbon level throughout the fouling layer is interesting.

One could imagine that the proteins would diffuse and be transferred out of the fouling layer as they are degraded. This does not appear to happen, and this implies that the mineral structure in some way is preventing the transport of the proteins. This strengthens the idea that the fouling consists of an interconnected network of proteins and minerals.

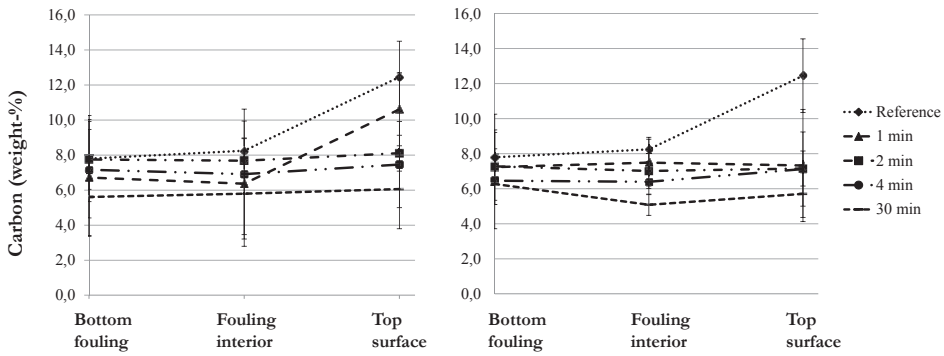

Figure 20 Results of the EDX measurements showing the changes in composition during cleaning in the cross-section of the fouling layer. The cleaning was performed for 0, 1, 2, 4 and 30 minutes in 1.5 wt% NaOH at a fluid velocity of 1.6 m/s. In the left panel, the experiment was perormed at 100°C, and in the right panel, it was perfomred at 120°C.

Structural changes in UHT fouling during cleaning

Some drastic change occurs to decrease the thickness measured by the laser triangulation sensor, while the relative concentration of the carbon source does not change. This could mean that lumps of fouling are detached from the surface, which would not have an impact on the overall percentage of the components. It could also mean that there are structural changes caused by the degradation of the protein part of the fouling network that have an impact on the thickness analysis. The latter is the more plausible explanation, since no dramatic eruption from the fouling layer was noted during the cleaning process.

As we have already observed from the top of the fouling in Figure 19, something does happen in the fouling structure closest to the bulk flow of the cleaning solution. It is not clear whether this change is due to a mass transfer of the deposit, to shrinkage of the structure or perhaps even to rearrangement of the proteins leading to a less opaque structure that could alter the reflectivity of the laser beam.

The structural effect of the alkali cleaning process is not easy to describe, although some effect can be seen from the top to the bottom of the fouling layer. The fouling in cross-section, before being exposed to the cleaning process, appears to be dense in large areas and only on a larger scale is the heterogeneity evident. In Figure 21A, one can see larger holes, and due to the properties of this heterogeneity, the structure can hold up to 60% water. The structure at the bottom of the fouling in cross-section appears very similar after cleaning, although small holes seem to penetrate the cleaned structure more frequently, and after 30 minutes (Figure 21C) there is a tendency towards more loose edges.

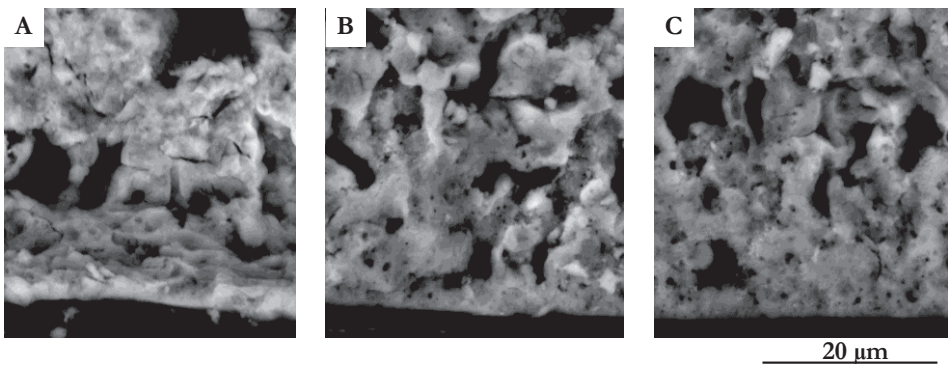

Figure 21 Bottom layer of the fouling that is situated closest to the metal surface. A, The reference, which has not been exposed to the cleaning process. B, The fouling after 8 minutes of cleaning with 1.5 wt% NaOH at 120°C and at a flow velocity of 1.6 m/s. C The fouling has been cleaned with the same settings of the cleaning parameters but for 30 minutes.

Closer to the bulk where the cleaning solution penetrates the fouling structure early in the process, SEM analysis reveals something interesting (Figure 22). The dense globular structure gradually changes into a hollow needle-like structure within the first few minutes of alkali treatment. The reasons for this change in structure are not completely understood. The structure seems to gain a translucent appearance, which would suggest diffusion of fouling away from the fouling layer. The remaining needle-like structure can also be compared to the calcium phosphate crystal structure formed at pH 6.25 in a bulk solution [45].

The overall composition of organic compounds does not seem to change drastically (Figure 20). Within the needle-like structure, it was difficult to determine accurately the composition. The reflecting volume of the EDX

measurement increases due to the porosity of the structure, which means that the results cannot be trusted for a specific structure at high magnification. By reducing the resolution and the energy of the x-ray beam, a better understanding of the composition of the needle-like structure might be possible.

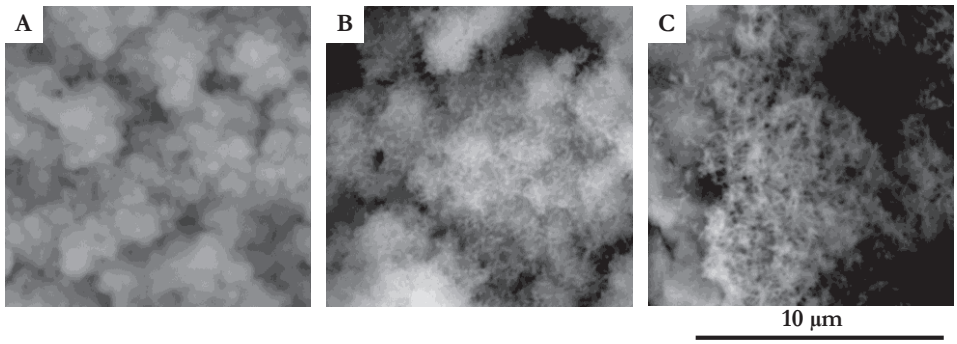

Figure 22 Images A to C show the degradation of the fouling layer during alkali cleaning. A, Fouling before cleaning; B, fouling that has been subjected to the cleaning process for 4 min at 120°C; and C, fouling that has been subjected to the cleaning process for 30 min at 100°C.

5.4 Cleaning efficiency and the parameters that influence the cleaning process

A discussion regarding the cleaning efficiency demands a definition of efficiency. In this work, the cleaning process is regarded as efficient when the UHT fouling is removed during the acid cleaning step and leaves behind a clean surface. The protein network has to be degraded sufficiently during the alkali cleaning to be disrupted and removed during the second acid cleaning step. If the process is not efficient, the protein network has not been degraded and a gel-like structure will remain (Figure 23). In Figure 23A, the time required to achieve a clean surface during the acid cleaning step is short compared to the inefficient cleaning shown in Figure 23B, where the process is both slow and inefficient.

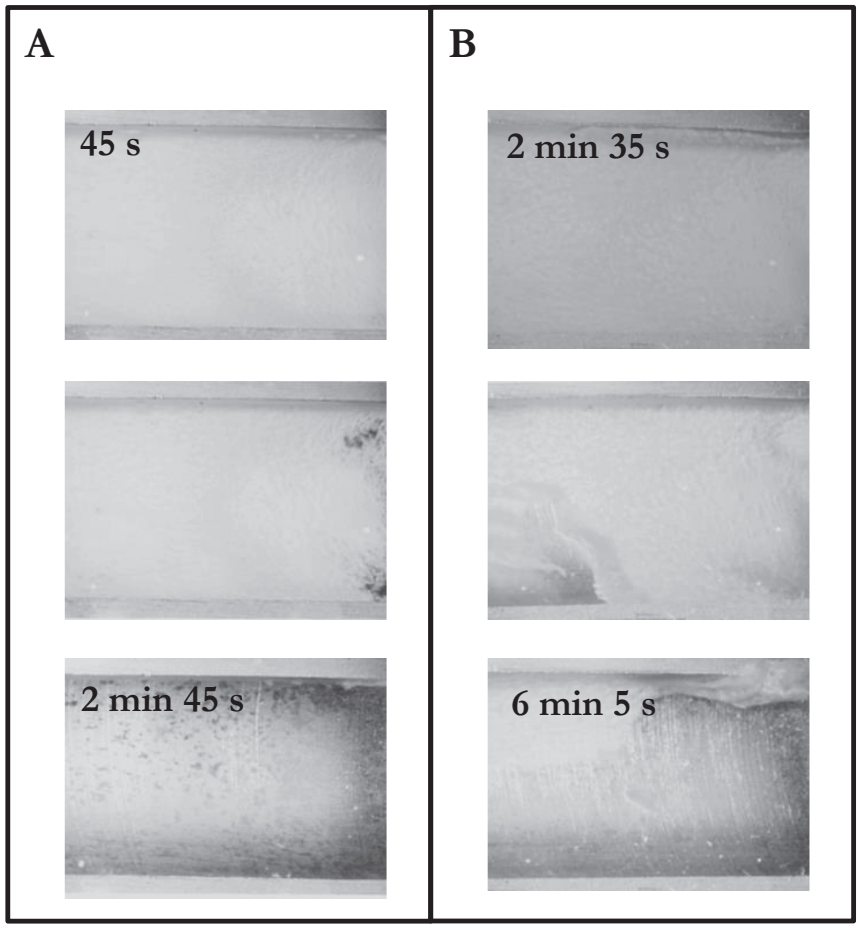

Figure 23 Two series of images showing the effect of acid cleaning after alkali cleaning. In A, efficient cleaning can be seen with a clean surface as the oucome, and B illustrates inefficient cleaning that leaves a protein gel on the surface.

The most radical inefficient cleaning can be visualized using a one-step cleaning process with acid (Figure 24). To gain a better understanding of what determines inefficient cleaning, the extreme case is relevant as a reference point. The figure shows the removal of mineral deposits after 1 and 4 minutes, respectively, and the scale at the side of each image shows the decreasing level of calcium in the fouling over time. An acid cleaning cycle that is not preceded by treatment will alkali will preserve the integrity of the structure of the protein network, while the mineral network will be transferred from the fouling layer.

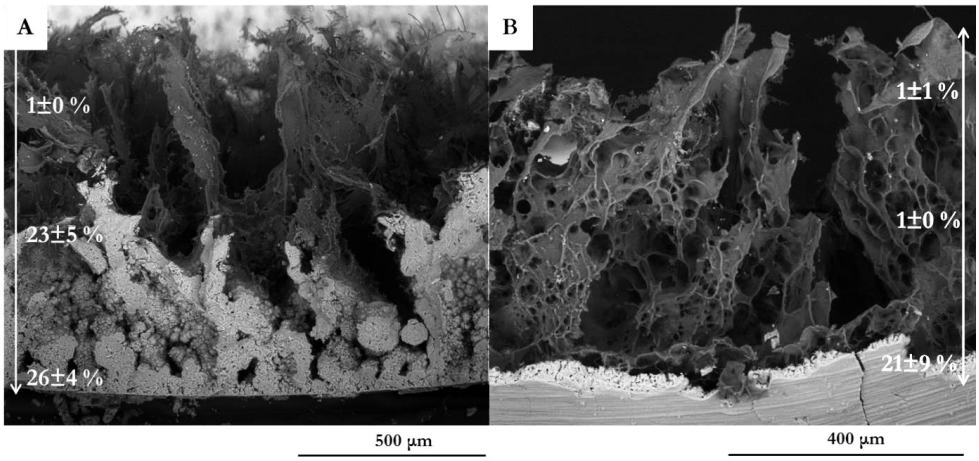

Figure 24 UHT fouling cleaned with acid without first being cleaned with alkali. A, Fouling after 1 minute; and B fouling after 4 minutes of cleaning. The calcium content is visualized as wt% of the dry weight at the side of each image.

The inefficient cleaning reveals some mechanistic features of the acid cleaning process. Even though the large structure in the fouling is heterogeneous with large structural variation, the mineral layer is being removed from the top down. The acid removal of calcium phosphate is rapid and the erosion from the top down in the fouling structure suggests a mechanism that is limited by the mass transfer of calcium phosphate from the surface.

An increase in flow velocity has been suggested to have an impact on cleaning efficiency for the model of removal of whey protein fouling under low flow velocity conditions. The swelling and reaction stage was found to be shortened and the removal stage was drastically decreased [70]. Flow velocities are difficult to compare between studies, since the shear forces from the flow, which are dependent upon the geometry of the cleaning vessel used, also have an impact on the cleaning. In this work, the velocity and the Reynold number were in the turbulent regime for all the velocities used, while most of the protein was not situated in a way that they it could be easily removed in the alkali cleaning step. Only the protein patches (Figure 10) were easily removed by the fluid flow (Figure 20).

The results from the cleaning trials show that the time needed for cleaning could be decreased by optimizing the cleaning parameters (Figure 25). By increasing the temperature from 100°C to 120°C, 12 minutes were saved during the alkali cleaning step. The degradation of the protein network was faster when the concentration of NaOH was increased from 1.5% to 3%, and this saved 4 minutes of cleaning time. The flow velocity did not have an impact on the degradation of the protein network or the time needed for cleaning.

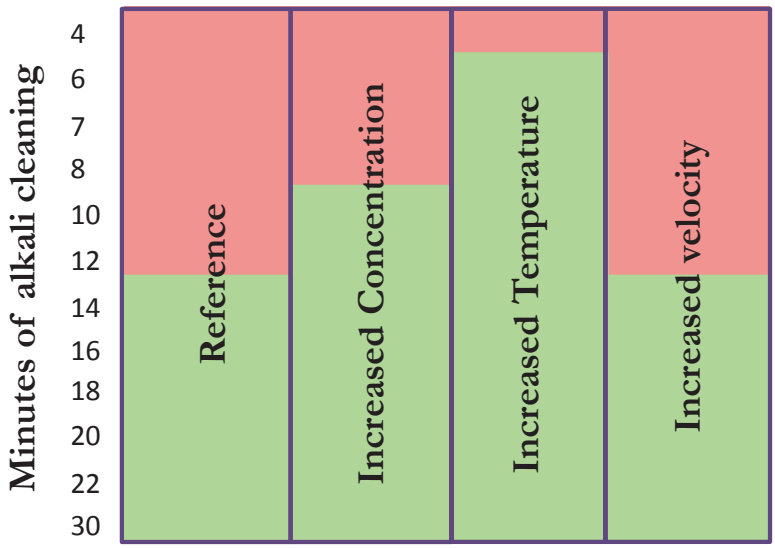

Figure 25 Summary of the results from the cleaning studies illustrating the effects of the different parameters of the alkali cleaning step on the efficiency of the process. The graph shows the number of minutes of alkali cleaning and the green areas indicate when the degree of depolymerization, i.e., degradation of the protein network, is sufficiently low for efficient cleaning in the final acid cleaning step. The parameters of temperature and concentration have the largest impacts.

5.5 Model of the cleaning process for the removal of UHT milk fouling

Investigating and understanding the structure and composition of the fouling could be have major implications for the accuracy of a cleaning model. UHT fouling has been shown to be a complex structure of interconnected protein and calcium phosphate networks. Even though the protein content is relatively low, it has been shown that it has a strong impact on the cleaning efficiency.

For the modelling done in this work, the degree of polymerization (DP) was used as a measure of cleaning efficiency (Paper IV). The limiting factor in the cleaning mechanism is not the transfer of proteins away from the fouling layer, but is rather the degradation of the protein matrix in the fouling layer.

To start from the beginning of the cleaning process, the convective mass transfer of hydroxyl ions and the diffusion of hydroxyl ions within the fouling layer have been used, as previously mentioned in Equations 5.2 to 5.6 (Chapter 5.1). Figure 26 shows that the diffusion through the fouling layer is expected to be rapid. Within 30 seconds, the concentration of hydroxyl ions inside the fouling layer is high. The shift to an efficient cleaning regime, where the surface is clean after the full CIP cycle, as discussed in Chapter 5.4 (Figure 25), occurs at between 12 and 14 minutes for the reference cleaning protocol. At these time-points, the concentration of hydroxyl ions is almost evenly distributed in the layer, as depicted by the red lines in Figure 26.

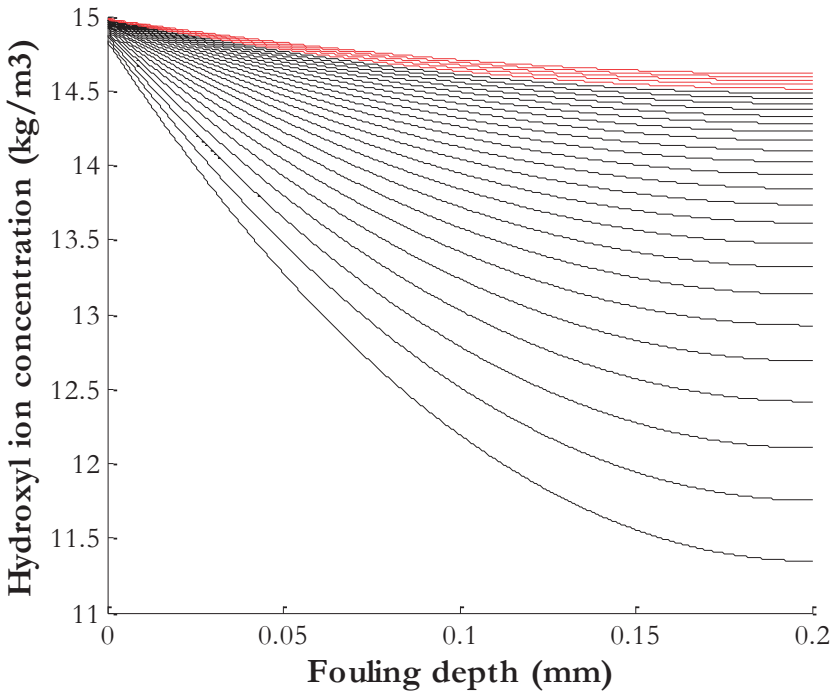

Figure 26 Graph illustrating the diffusion of hydroxyl ions in the fouling layer. The graph shows the concentration of hydroxyl ions (in kg/m^3) with respect to the depth of the fouling (in mm). Each line represents 30 seconds of alkali cleaning, and the red lines represent between 12 and 14 minutes of cleaning, corresponding to the shift in cleaning efficiency for the reference parameters.

Within the fouling layer, the alkali will react with the organic compounds, as discussed earlier in this chapter. The chemical reactions that occur are regarded as first-order reactions, where the DP is decreasing:

$$\frac{1}{DP_t} = \frac{1}{DP_0} + k * t \tag{5.7}$$

The rate coefficient of the cleaning reaction, k_r, is dependent upon the concentration of hydroxyl ions, c_{OH}, in the fouling

$$k_r = k' * {c_{OH}}^{0.6} * e^{-E_a/RT} \tag{5.8}$$

where k′ is the unknown reaction rate of the protein degradation. To be able to discuss the impacts of the different cleaning parameters, an arbitrary value was

assigned to k′ during the modeling. An activation energy (E_a) of 50 kJ/mol was found to describe ably the experimental data, which is similar to the previous data of Mercadé-Prieto et al. [83]

regarding cleaning with 0.35 M NaOH. They found the activation energies for the reaction to be between 45 kJ/mol and 72 kJ/mol and these are in the same range as for the breaking of the disulfide bond (76 kJ/mol). It should also be noted that 0.35 M NaOH is equivalent to the 1.5 wt% NaOH used as a reference concentration in the present work.

At a really high NaOH concentration of 0.87 M, which is a higher concentration than the 3 wt% used in this work, the activation energy was found to be about 150 kJ/mol, and this was explained by the collapse of the protein structure forming a gel from which the proteins had excessive difficulty to escape [83]. Even though the modeling data from the current study are to some extent consistent with literature data, the reactions that occur inside the UHT fouling are difficult to predict. The model of this system was applied using the COMSOL Multiphysics® 4.4 software. It was set up as 1-D problem and used 1334 elements across a 200-µm-thick deposit for calculating the hydroxyl ion diffusion, as described in detail in Paper IV.

In Figure 27, the alkali cleaning time is modeled in relation to the degree of polymerization (DP). The experimental results for cleaning efficiency show the inefficient alkali cleaning time marked in red and the efficient cleaning in green. The graph clearly shows that the degradation of the protein network needs to reach a certain level of DP in order to produce a clean surface at the end of the cleaning process. Experimental data have shown that the shift from an inefficient to efficient cleaning cycle occurs between 12 and 14 minutes for the reference cleaning cycle, corresponding to a DP of approximately 45%. Figure 27 can be used to relate the cleaning properties and DP to the reduction in time needed and the related energy savings in industry. This will be discussed further in Chapter 7.

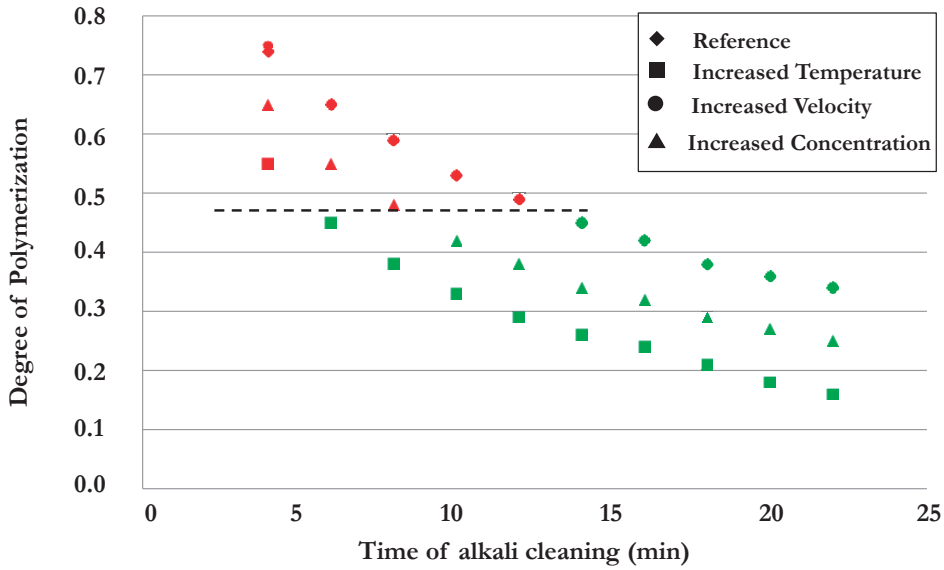

Figure 27 Modeled data for the change in degree of polymerization (DP) with alkali cleaning time. The reference protocol (100°C, 1.5% NaOH and flow velocity of 1.6 m/s) is compared to cases that use increased velocity (3 m/s), increased concentration of NaOH (3 wt%), and increased temperature (120°C). The shift from inefficient (red) to efficient (green) cleaning is adapted from experimental studies. At a DP of approximately 0.45, the end-result of the cleaning after the acid step will be a clean surface, whereas above this line the protein network will be strong enough to hinder its removal.

When the DP is decreasing, due to alkali cleaning, it affects the cleaning behavior during the acid cleaning. Figure 28 shows that the rate of cleaning during the acid step increases as the DP decreases. Therefore, the protein is thought to lose more and more of the interconnected network structure that keeps the structure together. This allows the degraded protein to follow when the mineral deposit is removed. Even though the acid cleaning process has been shown to be rapid under conditions of efficient DP, there is still some potential for saving a little time during the acid cleaning process by optimizing the conditions.

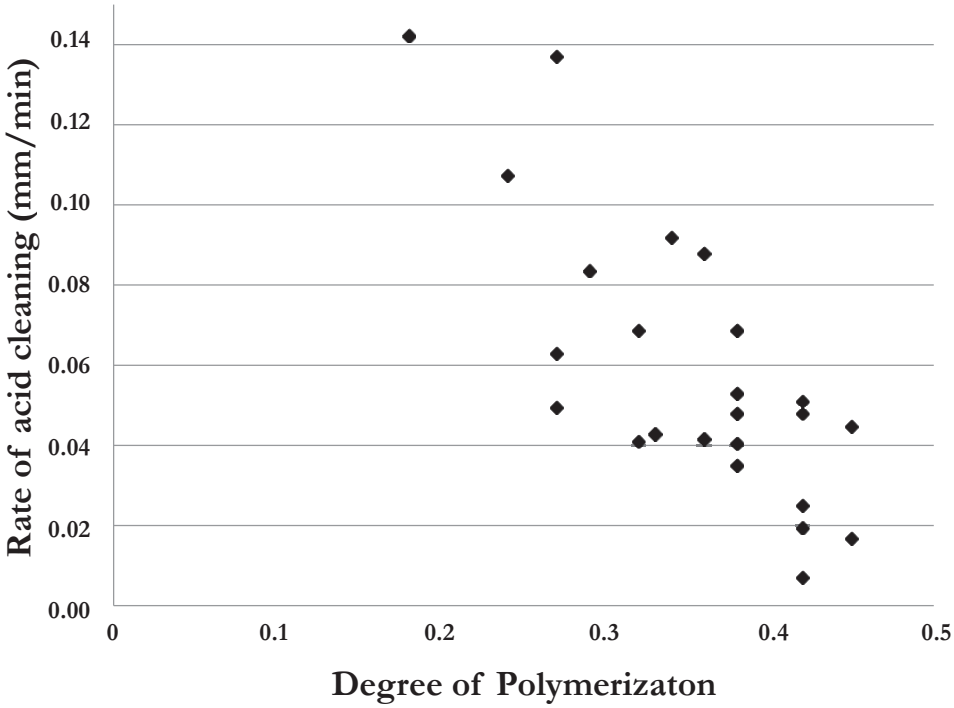

Figure 28 Experimental results on the acid cleaning rate (during efficient cleaning programs) in relation to the modeled data for degree of polymerization (DP). The decreasing DP has a positive effect on the rate of acid cleaning.

Summary

The pilot equipment that has been built during this work has the benefit of removing fouling layers under controlled settings for the cleaning process. The parameters that have been highlighted as relevant for the cleaning process are temperature, cleaning agent concentration, fluid velocity, and time, all of which are controlled and can be varied. A reference cleaning process of 1.5% NaOH at 100°C and fluid velocity of 1.6 m/s was conducted and compared to conditions with increased temperature, alkali concentration, and fluid velocity. The alkali cleaning step was followed by an acid cleaning step to reveal the impact of the alkali cleaning solution on the end result after an acid cleaning step.

The results of the cleaning were evaluated visually with a camera and by changes in fouling layer thickness using a laser triangulation sensor. After the first alkali cleaning, the fouling was investigated using SEM, CLSM and EDX. The duration of alkali cleaning was used as a measure of efficiency of the process. The cleaning process has been divided into two categories, efficient and inefficient cleaning. Efficient cleaning results in a clean surface, whereas inefficient cleaning leaves a gel-like structure of protein.

An alkali cleaning model shows that the cleaning process can be regarded as a process of depolymerization of the protein network inside the fouling layer, and a degree of polymerization of <0.45 results in an efficient cleaning process and a clean surface.

The mechanisms of cleaning can be summarized using a physical description of the cleaning process, as shown in Figure 29. In this model, the protein is shown in red and the mineral deposit in green. When the cleaning of UHT fouling begins with an alkaline cleaning agent, the depolymerization process starts as soon as the cleaning solution penetrates the fouling layer. The interpenetrated protein and mineral network is protected by the rigid mineral skeleton and no significant change in composition occurs.

However, the protein network is depolymerized, and when the acidic cleaning solution removes the rigid mineral structure the degree of polymerization will control whether the protein network remains intact or not. A low DP will allow for the second cleaning solution to remove the protein part of the fouling together with the minerals, leaving a clean surface. In the absence of an alkali cleaning step before the acid cleaning, the protein network will be intact and appear as a gel-like structure on the surface after cleaning.

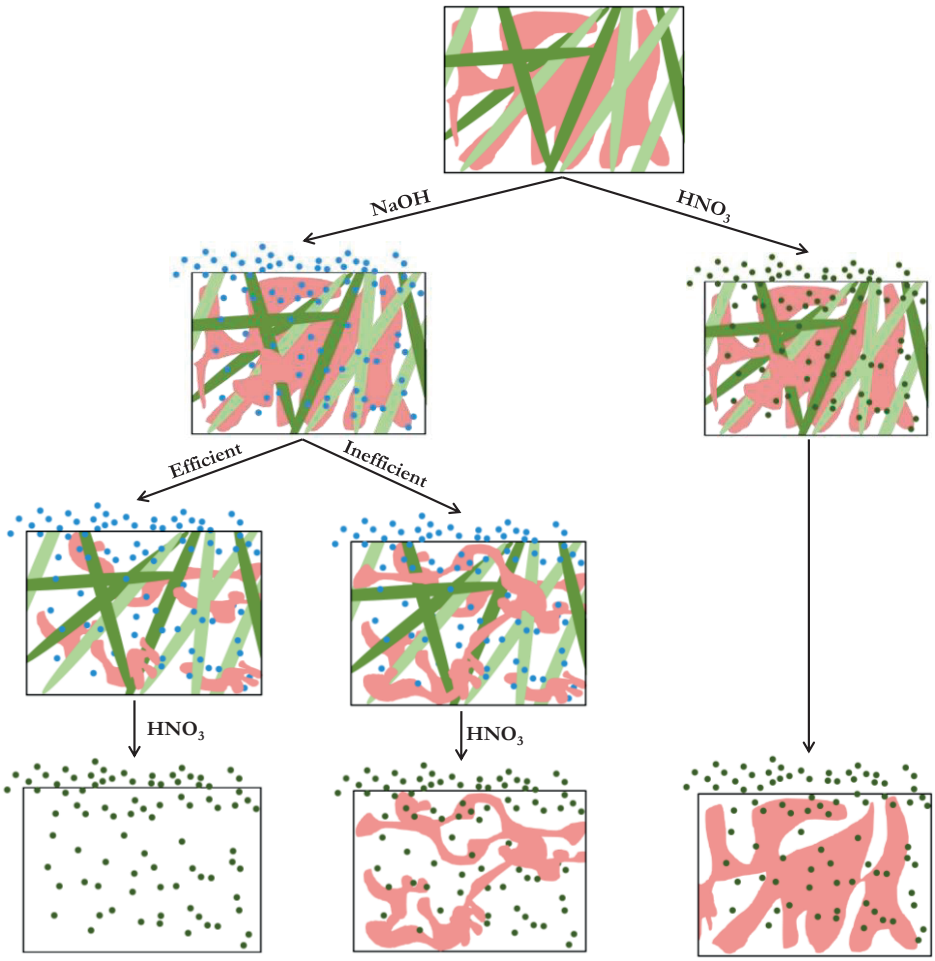

Figure 29 Physical model of the cleaning process to remove UHT fouling. The protein network is shown in read, and the mineral deposits are shown in green. The blue and green dots are alkali and acid cleaning agents, respectively. When alkali is used first, the cleaning can be divided into one efficient and one inefficient cleaning process, depending on the cleaning parameters used. Efficient cleaning removes the protein network togeteher with the mineral fraction during acid dissolution. In inefficient cleaning, the degree of polymerization (DP) is too high and this forms a strong protein network attached to the surface even after the cleaning process. The process is always inefficient when only an acid cleaning agent is used, and under these conditions the process leaves a gel-like stucture on the surface

6 Main Findings & Conclusions

The work of this thesis was performed to expand our knowledge of the structure, composition, and formation of UHT fouling and to understand how these properties affect the removal of fouling during the important cleaning process. The most important aspect of UHT fouling is that it consists of a mixed and interconnected network of proteins and minerals that creates a tough heterogeneous deposit on the heated surfaces. The aim of this work was to define the parameters of the cleaning process that have the highest impacts on the cleaning outcome. This will aid in tailoring the cleaning to ensure an efficient process with optimal usage of time, cleaning agents, and energy. The knowledge gained is summarized in a physical explanatory model that advances the research and understanding of UHT fouling.

One of the first conclusions to be drawn from the work of this thesis is that it is possible to create industrially relevant fouling under UHT conditions. It is also feasible to study the fouling layer in an online system with relevant cleaning parameters, and an experimental set-up that makes this possible is now available. The fouling formation process is designed to create many so-called coupons with fouling from the same batch, allowing good reproducibility for the analysis of cleaning behavior.

The chemical composition of the UHT fouling that we report agrees with previously reported data. In addition, we show that the structure and spatial distribution of the fully developed fouling layer are consistent. During alkali cleaning, the fouling takes on a translucent appearance but without the corresponding loss of protein. While the protein network is depolymerized, it is not removed from the rigid mineral structure. During acid cleaning, the mineral deposit is removed from the surface and takes with it the depolymerized protein network. The efficiency of UHT fouling cleaning is shown to be highly dependent upon the protein depolymerization that occurs during alkali cleaning, even though protein makes up only about 10% of the total fouling structure.

The investigations of the cleaning processes used for the removal of the UHT fouling permit a distinction to be drawn between efficient and inefficient cleaning processes. The efficiency of the CIP process cannot, with the chosen techniques, be visualized online during the alkali step; it is first seen during the acid cleaning step. Inefficient cleaning leaves enough of the protein network intact to allow a gel-like layer to remain on the surface after the minerals have been removed from the structure by the acid.

A new mechanistic model for cleaning has been developed, based on the understanding of the specific cleaning behavior of UHT fouling acquired in this study. A mathematical model has been designed that regards the cleaning efficiency during the alkali cleaning is determined as degradation or depolymerization of the protein network. The cleaning parameters of temperature and alkali cleaning agent concentration have the strongest impacts on the end result of two-step cleaning of UHT fouling. In this context, efficiency is taken as the reduction in time needed for cleaning, where a temperature increase saves almost 60% and an increase in NaOH concentration saves almost 30% of the time used, as compared to a reference process. Changing the fluid velocity within the turbulent regime does not have an impact on the time needed for alkali cleaning to achieve a clean surface in the subsequent acid cleaning step.

7 Application & Industrial Relevance

When translating the information and new knowledge gained in this work to an application it is important to remember dairies come in many different forms. For production efficiency reasons, all products are not produced at all locations. The production facilities specialize in different products, so the needs for cleaning also differ. By understanding the cleaning process and the mechanisms involved based on the information gained from analyses of structure and composition, the cleaning processes can be tailored for each individual unit.

The benefit gained by the industry from evaluating and using the new information on the structure and composition of the fouling layer could be very significant in terms of time and energy savings. This thesis shows that for UHT fouling, the temperature in the alkali cleaning step has the highest impact on the time required for efficient cleaning to be achieved. The second highest impact comes from the use of chemicals. These results are based solely on cleaning efficiency and point to the strong potential for reducing the total time need for the whole process. This reduction in time not only saves energy and chemicals, but can also be used to increase the effective production time.

To illustrate the impact of optimization of the cleaning parameters, we use the example of pilot plant fouling equipment with a 15-hour production period at a flow rate of 500 L/h. The cleaning process has a flow rate of 600 L/h. Efficient cleaning occurs when the polymerization of the protein network is decreased to at least 45%. The alkali cleaning in this example gives 30% protein polymerization, which corresponds to alkali cleaning for 27 min with the reference parameters of T = 100 °C and c = 1.5 wt% (Figure 27). The energy consumption is calculated taking into account that 40% of the heat is reused.

For a higher temperature (T = 120°C), approximately 0.4 hours of cleaning time per day could be saved, i.e., a reduction of 14 minutes for each cleaning process. This corresponds to an increase in production volume of 2.4% and an energy

saving of 3.6 kWh. The energy saved is approximately 30% of the total energy consumption for a cleaning process according to the reference parameters.

The concentration of cleaning agent is the second-best choice for optimizing the time perspective. Doubling the cleaning agent concentration from 1.5% to 3% decreases the time needed to reach efficient depolymerization of the protein network by 8 minutes, giving a saving in cleaning time of 0.3 hours per day. This confers a 2.1% increase in production volume and an energy saving of 5.2 kWh per day. The energy consumption is the same as that in the case with increased temperature, and it saves approximately 45% of the total energy used for cleaning. The fact that NaOH also has an increasing and negative environmental impact should also be taken into account.

Currently, in industry, more complex formulated products, which employ sequestering agents and surfactants to increase cleaning efficiency, are also used for the removal of UHT fouling. However, surfactants tend to be sensitive to higher temperatures and these solutions are often recommended to be used at temperatures <90°C, leaving the user with the option of varying the cleaning agent concentration, which is not optimal for UHT fouling removal. The use of a lower temperature could be beneficial in terms of energy use as long as the added cleaning agent compensates for the reduced cleaning efficiency of NaOH at this temperature. The hydroxyl ion concentration of commercially available cleaning solutions is within the range for optimal whey protein deposit removal (0.5 wt%), which means that an increase in temperature to the levels used in the present project would effectively reduce the hydroxyl concentration to approximately a third of what is shown here to be efficient within an acceptable time interval. Further investigations are needed to understand fully the impacts of formulated cleaning solutions on UHT fouling at industrially relevant temperatures and concentrations.

8 Future research

We have accumulated valuable knowledge on the structure and composition of the fully grown fouling layer from UHT processing, and we have shown how the fouling responds to a range of cleaning parameters. An experimental method for the formation of fouling under controlled and industrially relevant conditions is now available. It would be of great interest to study also the build-up of UHT fouling, to gain further insight into the driving force for layer build-up. This in turn would improve our understanding of the cleaning process and might suggest surface treatments that would prevent (or at least delay) the accumulation of this type of fouling.

With the equipment and measuring techniques that are now available, it will be of great interest to investigate the changes in both the growth and removal of fouling formed under different conditions. It would be of great value to build a knowledge-based map of fouling formed from different dairy products with different temperature intervals and with different compositions. The fouling map would need to be evaluated and complemented with a cleaning map. The cleaning would most likely show dependence on an increase in the levels of proteins or carbohydrates or a change in the mineral concentration. With a precise map of the fouling and cleaning behaviors for a wide range of fouling layers, further structured work with the cleaning parameters could be carried out. While the work of this thesis has looked at the cleaning parameters one at a time, the combined effect of the parameters that influence cleaning efficiency, as well as the consumption of energy, water, and chemicals would have a significant impact on efforts to create a dairy processing industry with lower environmental burden.

One cleaning approach that is currently used avoids the use of a pure alkali and a pure acid solution in the cleaning process. The detergent-manufacturing companies strive for formulated solutions with the combinatory effect of alkali and acid, together with agents that aid the removal of fouling. The new knowledge on the fouling structure and composition will help to guide the development of novel formulations of cleaning solutions.

Acknowledgments

I would first of all thank my main supervisor Tommy Nylander (LU[1]) and all of my co-supervisors: Marie Paulsson (LU), Christian Trägårdh (LU), Fredrik Innings (TPPS[2]), Lena Nilsson (Arla Foods), Michael Crafack (Arla Foods), Lars Hamberg (SP FB[3]), Niklas Lorén (SP FB) and Johan Wiklund (SP FB) for their support and valuable discussions throughout my work.

I would also like to acknowledge the financial support of TvärLivs, which is a co-operative venture between the Swedish Research Council Formas, Swedish Farmers Foundation for Agricultural Research (SLF), Swedish Governmental Agency for Innovation Systems Vinnova, Livsmedelsföretagen, and Svensk Dagligvaruhandel, as well as Tetra Pak Processing Systems and Arla Foods.

I would like to send my special thanks to Göran Pantzar (TPPS), Mikael Christensen (Arla Foods), Christian Sörensen (TPPS), and Steffen Øster Jensen (Arla Foods) for their invaluable and sometimes 24/7 support with my two pilot plants. Without you, this would have been 'mission impossible'.

Thank you Annika Altskär (SP FB) for spending so many hours with me in the windowless SEM room, with many fruitful discussions over sushi, and also for teaching me how to use the CLSM. I would like to thank Stefan Gustafsson (CTH[4]) for interesting discussions of my EDX analysis results and for being my interpretation guide.

I would like to thank all of my co-workers at SP Food and Bioscience, for creating a great and welcoming work place, with special thanks to the Department of

[1] LU – Lund University

[2] TPPS – Tetra Pak Processing Systems

[3] SP FB – Technical Research Institute of Sweden, Food and Bioscience

[4] CTH – Chalmers University of Technology

Process and Technology Development for the support and well-needed coffee break discussions and lunch walks, and to my roomies Emma and Lina for keeping me company.

To my division of Physical Chemistry at Lund University, thank you for always making me feel welcome, even though I only make short visits once every few months. Thank you James Holdaway (LU) for very interesting discussions, helping me out at the university and for lending me your video camera.

I would like to thank my diploma workers who have willingly tried out more or less crazy ideas over the years. Thank you Lasse, Idah, Cecilia, Jan-Maarten, Emelie, and Fredrik. Many thanks to the graduate school, LiFT, for interesting courses and exciting visits to industry and academic institutions. It has been great to meet with all of you in the PhD group over the years and to travel to new places, together with interesting discussions and gaining new perspectives.

Last but not least, I send my biggest thanks and love to my friends and my family. I believe you all know more about my PhD project than you would really want to, and I would like to thank you for listening to my endless monologues. Without you, this would never be. I love you!

References

1. Walstra, P., J.T.M. Wouters, and T.J. Geurts, *Milk*, in *Dairy Science and Technology, Second Edition*. 2005, CRC Press. p. 3-16.
2. Federation, I.D., *Bulletin of the IDF No. 481/2015 - The World Dairy Situation 2015*. 2015.
3. *Dairy Processing Handbook*. 2015 [cited 2015 12-07]; Available from: http://www.dairyprocessinghandbook.com/.
4. Gervind, P., et al., *Processintegrationsstudie - Värmepumpar inom mejeriprocessen Arla, Götene*. 2011, CIT Industriell Energi AB, SP Sveriges tekniska forskningsinstitut.
5. Alvarez, N., G. Daufin, and G. Gesan-Guiziou, *Recommendations for rationalizing cleaning-in-place in the dairy industry: case study of an ultra-high temperature heat exchanger.* Journal of dairy science, 2010. **93**(2): p. 808-21.
6. Federation, I.D., *Bulletin of the IDF No. 479/2015 - A common carbon footprint approach for the dairy sector - The IDF guide to standard life cycle assessment methodology*. 2015.
7. Walstra, P., J.T.M. Wouters, and T.J. Geurts, *Heat Treatment*, in *Dairy Science and Technology, Second Edition*. 2005, CRC Press. p. 225-272.
8. Walstra, P., J.T.M. Wouters, and T.J. Geurts, *Milk for Liquid Consumption*, in *Dairy Science and Technology, Second Edition*. 2005, CRC Press. p. 421-446.
9. Visser, J. and T.J.M. Jeurnink, *Fouling of heat exchangers in the dairy industry.* Experimental Thermal and Fluid Science, 1997. **14**(4): p. 407-424.
10. Welty, J.R., et al., *Fundamentals of Heat Transfer*, in *Fundamentals of Momentum, Heat, and Mass Transfer*. 2001, John Wiley & Sons, Inc. p. 201-214.
11. Asteriadou, K., et al., *Improving cleaning of industrial heat induced food an beverages deposits: a scientific approach to practice*, in *Proceedings of International Conference on Heat Exchanger Fouling and Cleaning VIII*. 2009: Schladming, Austria. p. 158-164.
12. Grijspeerdt, K., *Applications of modelling to optimise ultra high temperature milk heat exchangers with respect to fouling.* Food Control, 2004. **15**(2): p. 117-130.
13. Christian, G.K. and P.J. Fryer, *The Effect of Pulsing Cleaning Chemicals on the Cleaning of Whey Protein Deposits.* Food and Bioproducts Processing, 2006. **84**(4): p. 320-328.

14. Burton, H., *Deposits from Milk in Heat Treatment Plants - a Review and Discussion.* Journal of Dairy Research, 1968. **35**: p. 317-330.
15. Jimenez, M., et al., *Toward the understanding of the interfacial dairy fouling deposition and growth mechanisms at a stainless steel surface: A multiscale approach.* Journal of Colloid and Interface Science, 2013. **404**(0): p. 192-200.
16. Lalande, M., J.P. Tissier, and G. Corrieu, *Fouling of a plate heat exchanger used in ultra-high-temperature sterilization of milk.* Journal of Dairy Research, 1984. **51**: p. 557-568.
17. Lyster, R.L.J., *The composition of milk deposits in an ultra-high-temperature plant.* Journal of Dairy Research, 1965. **32**: p. 203-208.
18. Schraml, J.E. and H.G. Kessler. *Effects on concentration on fouling at hot surfaces*. in *Fouling and Cleaning in Food Processing*. 1994. Jesus College, Cambridge.
19. Walstra, P., J.T.M. Wouters, and T.J. Geurts, *Milk Components*, in *Dairy Science and Technology, Second Edition*. 2005, CRC Press. p. 17-108.
20. Holt, C., et al., *Invited review: Caseins and the casein micelle: Their biological functions, structures, and behavior in foods1.* Journal of Dairy Science, 2013. **96**(10): p. 6127-6146.
21. Belitz, H.-D., W. Grosch, and P. Schieberle, *Milk and Dairy Products*, in *Food Chemistry*. 2004, Springer. p. 471-512.
22. McSweeney, P.L.H. and P.F. Fox, *Advanced dairy chemistry [Elektronisk resurs] : Volume 1A, Proteins: basic aspects, 4th Edition*. 2013, Boston, MA: Springer US :.
23. Dalgleish, D.G., *On the structural models of bovine casein micelles-review and possible improvements.* Soft Matter, 2011. **7**(6): p. 2265-2272.
24. Holt, C., et al., *Substructures of bovine casein micelles by small-angle X-ray and neutron scattering* Colloids and Surfaces A: Physicochemical Eng. Aspects, 2003. **213**: p. 275-284.
25. Dalgleish, D.G. and A.J.R. Law, *pH-Induced dissociation of bovine casein micelles. I. Analysis of liberated caseins.* Journal of Dairy Research, 1988. **55**(04): p. 529-538.
26. O'Connell, J.E. and P.F. Fox, *Effect of β-lactoglobulin and precipitation of calcium phosphate on the thermal coagulation of milk.* Journal of Dairy Research, 2001. **68**(01): p. 81-94.
27. Little, E. and C. Holt, *An equilibrium thermodynamic model of the sequestration of calcium phosphate by casein phosphopeptides.* European Biophysics Journal, 2004. **33**(5): p. 435-447.
28. Beliciu, C.M., A. Sauer, and C.I. Moraru, *The effect of commercial sterilization regimens on micellar casein concentrates.* Journal of Dairy Science, 2012. **95**(10): p. 5510-5526.
29. Dalgleish, D.G., H.D. Goff, and B. Luan, *Exchange reactions between whey proteins and caseins in heated soya oil-in-water emulsion systems — behavior of individual proteins.* Food Hydrocolloids, 2002. **16**(4): p. 295-302.

30. Huppertz, T. and A.L. Kelly, *Properties and constituents of cow's milk*, in *Milk Processing and Quality Management*. 2009, John Wiley & Sons. p. 23-47.
31. Jelen, P. and W. Rattray, *Thermal denaturation of whey protein*, in *Heat-Induced Changes in Milk*, P.F. Fox, Editor. 1995, International Dairy Federation: 41, Square Vergote, B-1040 Brussels. p. 66-85.
32. de Wit, J.N., *Thermal behaviour of bovine β-lactoglobulin at temperatures up to 150°C. a review.* Trends in Food Science & Technology, 2009. **20**(1): p. 27-34.
33. Tolkach, A. and U. Kulozik, *Reaction kinetic pathway of reversible and irreversible thermal denaturation of β-lactoglobulin.* Lait, 2007. **87**: p. 301-315.
34. Langton, M. and A.-M. Hermansson, *Fine-stranded and particulate gels of beta-lactoglobulin and whey protein at varying pH.* Food Hydrocolloids, 1992. **5**(6): p. 523-539.
35. Petit, J., et al., *Influence of calcium on β-lactoglobulin denaturation kinetics: Implications in unfolding and aggregation mechanisms.* Journal of Dairy Science, 2011. **94**: p. 5794-5810.
36. Blanpain-Avet, P., et al., *Analysis by Raman spectroscopy of the conformational structure of whey proteins constituting fouling deposits during the processing in a heat exchanger.* Journal of Food Engineering, 2012. **110**: p. 86-94.
37. Khaldi, M., et al., *Effect of calcium content and flow regime on whey protein fouling and cleaning in a plate heat exchanger.* Journal of Food Engineering, 2015. **147**(0): p. 68-78.
38. Christian, G.K., S.D. Changani, and P.J. Fryer, *The Effect of Adding Minerals on Fouling from Whey Protein Concentrate.* Food and Bioproducts Processing, 2002. **80**(4): p. 231-239.
39. Gaucheron, F., *The minerals of milk.* Reproduction Nutrition Development, 2005. **45**(4): p. 473-483.
40. Morison, K.R. and S.H. Tie, *The Development and Investigation of a Model Milk Mineral Fouling Solution.* Food and Bioproducts Processing, 2002. **80**(4): p. 326-331.
41. Pouliot, Y., M. Boulet, and P. Paquin, *Observations on the heat-induced salt balance changes in milk I. Effect of heating time between 4 and 90 degrees.* Journal of Dairy Research, 1988. **56**: p. 185-192.
42. Gebauer, D., et al., *Pre-nucleation clusters as solute precursors in crystallisation.* Chemical Society Reviews, 2014. **43**(7): p. 2348-2371.
43. Evans, D.F. and H. Wennerström, in *The colloidal domain. Where physics, chemistry, biology and technology meet*

1999, Wiley-VCH. p. 401-437.
44. On-Nom, N., A.S. Grandison, and M.J. Lewis, *Measurement of ionic calcium, pH, and soluble divalent cations in milk at high temperature.* Journal of Dairy Science, 2010. **93**(2): p. 515-523.

45. Andritsos, N., S.G. Yiantsios, and A.J. Karabelas, *Calcium Phosphate Scale Formation from Simulated Milk Ultrafiltrate Solutions.* Food and Bioproducts Processing, 2002. **80**(4): p. 223-230.
46. Rosmaninho, R. and L.F. Melo, *The effect of citrate on calcium phosphate deposition from simulated milk ultrafiltrate (SMUF) solution.* Journal of Food Engineering, 2006. **73**: p. 379-387.
47. Bird, M.R. and P.J. Fryer, *Experimental study of cleaning of surfaces fouled by whey proteins.* Food and Bioproducts Processing, 1991. **69**: p. 13-21.
48. Holt, C., *Effect of heating and cooling on the milk salts and their interaction with casein*, in *Heat-Induced Changes in Milk*, P.F. Fox, Editor. 1995, International Dairy Federation: 41, Square Vergote, B-1040 Brussels. p. 105-133.
49. O'Brien, *Heat Induced Changes in Lactose: Isomerization, Degradation, Maillard Browning*, in *Heat-Induced Changes in Milk* P.F. Fox, Editor. 1995, International Dairy Federation: 41, Square Vergote, B-1040 Brussels. p. 134-170.
50. Fox, P.F. and P.L.H. McSweeney, *Milk Lipids*, in *Dairy Chemistry and Biochemistry*. 1998, Thomson Science, Kluwer Academic Publishers Group. p. 67-145.
51. Dewettinck, K., et al., *Nutritional and technological aspects of milk fat globule membrane material.* International Dairy Journal, 2008. **18**(5): p. 436-457.
52. Foster, C.L. and M.L. Green, *A model heat exchange apparatus for the investigation of fouling of stainless steel surfaces by milk II. Deposition of fouling material at 140 °C, its adhesion and depth profiling.* Journal of Dairy Research, 1990. **57**: p. 339-348.
53. Prakash, S., O. Kravchuk, and H. Deeth, *Influence of pre-heat temperature, pre-heat holding time and high-heat temperature on fouling of reconstituted skim milk during UHT processing.* Journal of Food Engineering, 2015. **153**(0): p. 45-52.
54. Tissier, J.P. and M. Lalande, *Experimental Device and Methods for Studying Milk Deposit Formation on Heat Exchange Surfaces.* Biotechnology Progress, 1986. **2**(4): p. 218-229.
55. Bouman, S., F.M. Driessen, and D.G. Schmidt. *Growth of thermoresistant Streptococci and deposition of milk on the plates of heat exchangers during long running times*. in *Fundamentals and Applications of Surface Phenomena Associated with Fouling and Cleaning in Food Processing*. 1981. Tylösand, Sweden.
56. Goldstein, J.I., *Scanning electron microscopy and x-ray microanalysis*. 2003, New York: Kluwer Academic / Plenum.
57. Jones, D.B., *Factors for converting percentages of nitrogen in foods and feeds into percentages of proteins*, U.S.D.o. Agriculture, Editor. 1941: Washington, D.C.

58. Abhyankar, A.R., D.M. Mulvihill, and M.A.E. Auty, *Combined confocal microscopy and large deformation analysis of emulsion filled gels and stirred acid milk gels.* Food Structure, 2014. **1**(2): p. 127-136.
59. Wright, S.J. and D.J. Wright, *Chapter 1 - Introduction to Confocal Microscopy*, in *Methods in Cell Biology*, M. Brian, Editor. 2002, Academic Press. p. 1-85.
60. Leica. *True Confocal Scanner Leica TCS SP II - User manual*. [cited 2015 12-09]; RK09052000:[Available from: http://www.leica-microsystems.com/fileadmin/downloads/Leica%20TCS%20SP2/User%20Manuals/TCS_SP2_09052000_english.pdf.
61. Angel Rufián-Henares, J., E. Guerra-Hernández, and B. García-Villanova, *Available lysine and fluorescence in heated milk proteins/dextrinomaltose or lactose solutions.* Food Chemistry, 2006. **98**(4): p. 685-692.
62. Francis-Lang, H., et al., *Live Confocal Analysis with Fluorescently Labeled Proteins*, in *Confocal Microscopy Methods and Protocols*, S. Paddock, Editor. 1999, Humana Press. p. 223-239.
63. Paredes, R.M., et al., *Chemical calcium indicators.* Methods, 2008. **46**(3): p. 143-151.
64. McIntosh, A.O. and W.L. Jablonski, *X-Ray Diffraction Powder Patterns of Calcium Phosphates.* Analytical Chemistry, 1956. **28**(9): p. 1424-1427.
65. Mekmene, O., et al., *Effects of pH and Ca/P molar ratio on the quantity and crystalline structure of calcium phosphates obtained from aqueous solutions.* Dairy Science & Technology, 2009. **89**(3-4): p. 301-316.
66. Guyomarc'h, F., et al., *Role of the Soluble and Micelle-Bound Heat-Induced Protein Aggregates on Network Formation in Acid Skim Milk Gels.* Journal of Agricultural and Food Chemistry, 2003. **51**(26): p. 7743-7750.
67. Fryer, P.J. and K. Asteriadou, *A prototype cleaning map: A classification of industrial cleaning processes.* Trends in Food Science & Technology, 2009. **20**(6-7): p. 255-262.
68. Liu, W., et al., *Direct measurement of the force required to disrupt and remove fouling deposits of whey protein concentrate.* International Dairy Journal, 2006. **16**(2): p. 164-172.
69. Liu, W., et al., *Identification of cohesive and adhesive effects in the cleaning of food fouling deposits.* Innovative Food Science and Emerging Technologies, 2006. **7**(4): p. 263-269.
70. Xin, H., X.D. Chen, and N. Özkan, *Removal of a model protein foulant from metal surfaces.* AIChE Journal, 2004. **50**(8): p. 1961-1973.
71. Christian, G.K. and P.J. Fryer, *The balance between chemical and physical effects in the cleaning of milk fouling deposits*, in *ECI Conference on Heat Exchanger Fouling and Cleaning: Fundamentals and Applications*. 2003: New Mexico, USA p. Article 23.
72. Littlejohn, F., C.S. Grant, and A.E. Sáez, *Mechanisms for the Removal of Calcium Phosphate Deposits in Turbulent Flow.* Industrial & Engineering Chemistry Research, 2000. **39**(4): p. 933-942.

73. Lee, S.H. and J.C. Rasaiah, *Proton transfer and the mobilities of the H+ and OH- ions from studies of a dissociating model for water.* Journal of Chemical Physics, 2011. **135**(12): p. 124505.
74. Galani, D. and R.K. Owusu Apenten, *Heat-induced denaturation and aggregation of β-lactoglobulin: Kinetics of formation of hydrophobic and disulphide-linked aggregates.* International Journal of Food Science and Technology, 1999. **34**(5-6): p. 467-476.
75. Jeurnink, T.J.M. and D.W. Brinkman, *The cleaning of heat exchangers and evaporators after processing milk or whey.* International Dairy Journal, 1994. **4**(4): p. 347-368.
76. Gallot-Lavallee, T. and M. Lalande, *A mechanistic approach of pasteurized milk deposit cleaning*, in *Fouling & Cleaning in Food Processing*, D. Lund, E. Plett, and C. Sandu, Editors. 1985: University of Wisconsin-Madison. p. 374-394.
77. Saikhwan, P., et al., *Swelling and dissolution in cleaning of whey protein gels.* Food and Bioproducts Processing, 2010. **88**(4): p. 375-383.
78. Mercadé-Prieto, R., et al., *Swelling and Dissolution of â-Lactoglobulin Gels in Alkali.* Biomacromolecules, 2007. **8**: p. 469-476.
79. Xin, H., X.D. Chen, and N. Özkan, *Whey Protein-Based Gel as a Model Material for Studying Initial Cleaning Mechanisms of Milk Fouling.* Journal of Food Science, 2002. **67**(7): p. 2702-2711.
80. Tuladhar, T., W. Paterson, and D. Wilson, *Investigation of Alkaline Cleaning-in-Place of Whey Protein Deposits Using Dynamic Gauging.* Food and Bioproducts Processing, 2002. **80**(3): p. 199-214.
81. Mercadé-Prieto, R., et al., *Effect of Gel Structure on the Dissolution of Heat-Induced β-Lactoglobulin Gels in Alkali.* Journal of Agricultural and Food Chemistry, 2006. **54**(15): p. 5437-5444.
82. Fryer, P.J., P.T. Robbins, and K. Asteriadou, *Current knowledge in hygienic design: can we minimize fouling and speed cleaning?* Procedia Food Science, 2011. **1**(0): p. 1753-1760.
83. Mercadé-Prieto, R., D.I. Wilson, and W.R. Paterson, *Effect of the NaOH Concentration and Temperature on the Dissolution Mechanisms of ß-Lactoglobulin Gels in Alkali.* International Journal of Food Engineering, 2008. **4**(5): p. Article 9.
84. Grant, C.S., G.E. Webb, and Y.W. Jeon, *A Noninvasive study of milk cleaning processes: calcium phosphate removal.* Journal of Food Process Engineering, 1997. **20**(3): p. 197-230.
85. Alvarez, N., G. Gesanguiziou, and G. Daufin, *The role of surface tension of re-used caustic soda on the cleaning efficiency in dairy plants.* International Dairy Journal, 2007. **17**(4): p. 403-411.

Printed by Media-Tryck, Lund University, Sweden

När mjölk processas i mejeriindustrin bildas en beläggning på de värmande ytorna som kallas fouling. Fouling byggs upp av en blandning av proteiner och mineraler. Anledningen till att dessa fastnar på ytorna är att de reagerar på värmen i anläggningen. Beläggningen hindrar värmen från att transporteras in i mjölken och måste därför diskas bort innan den blir för tjock, för att försäkra att all mjölk värms upp till samma temperatur.

Kalcium som finns i hög koncentration i mjölk har en egenskap som gör att den löser sig mindre och mindre när temperaturen i mjölken höjs. Därför återfinns en ökad mineralkoncentration i fouling som producerats vid höga temperaturer. Den fouling som har studerats i detta arbete är producerad vid vad som brukar kallas för ultra-hög temperatur eller UHT. UHT-mjölk har en lång hållbarhet och kan förvaras i rumstemperatur. Strukturen och sammansättningen på den fouling som bildas under denna värmeprocess har noga studerats i projektet för att bättre förstå vad som händer under rengöringen av processanläggningen.

Genom att studera vad som händer under diskprocessen kan förståelse nås kring hur processen kan påverkas och optimeras. De viktigaste parametrarna att förstå är vid vilken temperatur som det är bäst att diska, hur snabbt disklösningen måste flöda över beläggning, vilken koncentration disklösningen behöver ha och hur lång tid som behövs för att ytan ska bli ren. Genom att justera dessa parametrar går det att minska användningen av energi, vatten och diskkemikalier. Resultaten av arbetet är användbara för industrin för att kunna skräddarsy ett system för disken som är mest effektiv för just den anläggningen och den speciella produkten.

LUND UNIVERSITY

ISBN 978-91-7422-429-0

Doctoral Thesis
Physical Chemistry
Lund University